2

Radio Channel Characterisation

Jørgen Bach Andersen, Aalborg University, Denmark

The properties of the time varying, frequency dispersive radio channel used for mobile and personal communications are important to know for several reasons. There are scientific reasons for understanding the phenomena involved, and there are practical reasons for being able to design optimal communications networks which have the best possible signal strength and quality for a multi-user situation. In COST 231 Working Group 2 on UHF propagation a number of collaborative results have been achieved, which are described in Chapters 2, 3 and 4.

Specifically, Chapter 2 focuses on the theoretical basis for describing the instantaneous and average quantities are given, as well as measurement techniques and results, and methods for simulating the mobile channel.

In the following Chapter 3, novel results for antennas are described, both for the base station and the portable unit. For the base station diversity systems play an important role, both micro- and macro diversity, while for the portable antennas problems like absorption in the user have been addressed.

Finally, Chapter 4 describes the results of modelling the pathloss and time dispersion for rural, micro cells and indoor situations. It is especially significant that a number of theoretical models have been compared with the same reference experimental situation, making comparisons possible. In the last section, models for penetration into buildings and propagation in special environments (such as tunnels) have been addressed.

2.1 Characteristics of radio channels

Bernard Fleury, Swiss Federal Institute of Technology, Switzerland

In the mobile radio environment, a part of the electromagnetic energy radiated by the antenna of the transmitting station reaches the receiving station by propagating through different paths. Along these paths, interactions which are commonly referred to as propagation mechanisms, may occur between the electromagnetic field and various objects. Possible interactions are specular reflection on large plane surfaces, diffuse scattering from surfaces exhibiting small irregularities or from objects of small size, transmission through dense material like walls or floors, shadowing by obstacles like trees, etc. The attributes small and large are to be understood here with respect to the wavelength. A detailed description of these propagation mechanisms is given in Chapter 4, Section 4.3.

During the last few years, attention in the research field of propagation prediction and to some extent in the area of propagation simulation has been increasingly focused on issues concerning the resolution of the electric field with respect to both the propagation delay and the incidence direction (cf. e.g. [1], [2]). The characterisation given below accounts for this development in the sense that it relies on the notion of the field direction-delay-spread function.

2.1.1 Field Direction-Delay-Spread Function

For the subsequent discussion it is worth regarding the impinging waves as being radiated by sources which are distributed in the surroundings of the receiver. Due to the different positions of these sources, the resulting electric field at the receiver position is spread both in time and in direction. The dispersive nature of the environment is characterised by the location-dependent direction-delay-spread function (DDSF) $\dot{E}(\dot{z},\Omega,\tau)$ of the electric field vector. Here, $\dot{z}$ denotes the receiver position with respect to an arbitrary co-ordinate system with origin O_{ref} (see Fig. 2.1). The element Ω of the sphere S of arbitrary radius uniquely characterises the incidence direction (see Fig. 2.2) and τ stands for the delay variable. The spherical co-ordinates ϕ (longitude) and θ (colatitude) uniquely determine the direction Ω, and conversely.

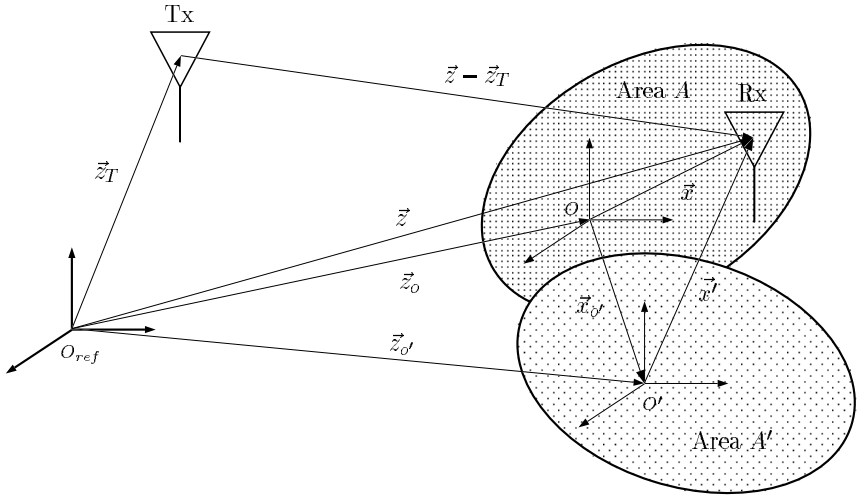

Fig. 2.1 Geometrical situation considered.

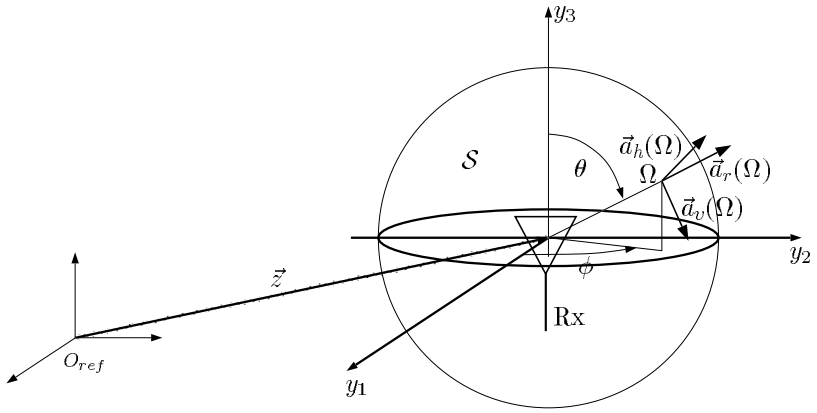

Fig. 2.2 Definition of the direction Ω and its associated unit vectors $\bar{a}_r(\Omega), \bar{a}_h(\Omega), \bar{a}_v(\Omega)$.

Assumption I: The receiver is located in the far-field region of the radiating sources.

As a consequence, the impinging waves are transverse electromagnetic. Their electric field vector $\dot{\bar{E}}(\dot{z}, \Omega, \tau)$ lies in the plane spanned by the unit normal vectors $\bar{a}_h(\Omega)$

and0 $\bar{a}_v(\Omega)$. Accordingly, denoting with $E_{h|v}(\dot{z},\Omega,\tau)$ the horizontal | vertical component of $\dot{E}(\dot{z},\Omega,\tau)$, the following relationships may be written: $\dot{E}(\dot{z},\Omega,\tau) = E_h(\dot{z},\Omega,\tau)\dot{a}_h(\Omega) + E_v(\dot{z},\Omega,\tau)\dot{a}_v(\Omega)$. Then, let $E(\dot{z},\Omega,\tau) := \left[E_h(\dot{z},\Omega,\tau), E_v(\dot{z},\Omega,\tau)\right]^T$ be the field DDSF (FDDSF) at location $\dot{z}$, where $[\cdot]^T$ stands for the transposition operation. Depending on the kind of interactions along the propagation paths, the FDDSF may embody a coherent and a diffuse part, i.e., it can be written as

$$E(\bar{z},\Omega,\tau) = E_c(\bar{z},\Omega,\tau) + E_d(\bar{z},\Omega,\tau), \tag{2.1}$$

where $E_d(\bar{z},\Omega,\tau)$ is a regular vector-valued function, while $E_c(\bar{z},\Omega,\tau)$ is a sum of weighted Dirac measures:

$$E_c(\dot{z},\Omega,\tau) = \sum_{j=1}^{J(\bar{z})} E_j(\dot{z})\,\delta(\Omega-\Omega_j(\dot{z}))\,\delta(\tau-\tau_j(\dot{z})). \tag{2.2}$$

The FDDSF can also be decomposed into a sum of components each being contributed by a specific radiating source:

$$E(\dot{z},\Omega,\tau) = \sum_{\text{r}=1}^{L(\bar{z})} E_{\text{r}}(\dot{z},\Omega,\tau). \tag{2.3}$$

As the location changes over small areas not larger than some tens of the wavelength, the components in (2.3) exhibit rapid fluctuations in amplitude and phase which are called small-scale variations or small-scale fading. As the receiver moves over larger areas, the distance and the direction of the radiating sources vary with respect to its instantaneous location. Consequently, their corresponding component in the FDDSF drifts in the (Ω,τ)-space as a function of $\dot{z}$. Moreover, some radiating sources may be partly obstructed or disappear while new ones may arise, e.g., in transition regions from a line-of-sight (LOS) to a non-line-of-sight (NLOS) situation or vice-versa. Thus, some components in (2.3) may be attenuated or vanish and new ones may appear. The variations due to location changes over wider areas are called large-scale fluctuations or large-scale fading.

2.1.2 Space-Dependent Channel Impulse Response

The radio channel incorporates the propagation medium as well as the transmitting and receiving antennas. Its response is given up to a proportionality constant C which

depends on the antenna characteristics from integrating the FDDSF weighted by the antenna field pattern with respect to the direction:

$$h(\dot{z},\tau) := C\int f(\Omega)^T E(\dot{z},\Omega,\tau)d\Omega.$$

Here, $f(\Omega)$ is the electric field pattern of the receiving antenna, i.e., $f(\Omega) = \left[f_h(\Omega), f_v(\Omega) \right]^T$. The channel impulse response (CIR) is equal to $\frac{1}{P_T} h(\dot{z},\tau)$, where P_T is the power at the input of the transmitter antenna. According to common practice, $h(\bar{\dot{z}},\tau)$ is also referred to as the CIR in the sequel. It essentially retains the features of the FDDSF regarding the short-term and large-scale fluctuations and its decomposition into a coherent and a diffuse part as

$$h(\bar{\dot{z}},\tau) = h_c(\bar{\dot{z}},\tau) + h_d(\bar{\dot{z}},\tau) \tag{2.4}$$

with $h_c(\dot{z},\tau) = C\sum_{j=1}^{J(\bar{\dot{z}})} f(\Omega_j(\dot{z}))^T E_j(\dot{z})\delta(\tau - \tau_j(\dot{z}))$ and $h_d(\dot{z},\tau) = C\int f(\Omega)^T E_d(\dot{z},\Omega,\tau)d\Omega$ or into the sum of the components corresponding to the radiating sources according to $h(\dot{z},\tau) = \sum_{\nu=1}^{L(\bar{\dot{z}})} h_\nu(\dot{z},\tau)$ with

$$h_\nu(\dot{z},\tau) = C\int f(\Omega)^T E_\nu(\dot{z},\Omega,\tau)d\Omega. \tag{2.5}$$

2.1.3 Time-Dependent Channel Response

When the receiver moves along a trajectory $\bar{\dot{z}}(t)$, the channel varies with time. Its time-variant response is given as

$$h(t,\tau) := h(\bar{\dot{z}}(t),\tau). \tag{2.6}$$

Notice that strictly speaking the widely used expression time-variant impulse response is not appropriate for $h(t,\tau)$ because this function is not the response of the channel to an impulse at a certain instant. The time fluctuations of the channel response (CR) which result from the small-scale and large-scale variations are referred to as short-term and long-term variations or fading, respectively. Studies of the time-variant radio channel traditionally rely on the assumption that the temporal fluctuations exclusively

result from receiver displacements with constant velocity, i.e., the receiver trajectory is of the form

$$\bar{z}(t) = \bar{z}_0 + \bar{v}t. \tag{2.7}$$

In this case, $h(t,\tau)$ reflects up to the time scaling factor $\|\bar{v}\|$ the spatial behaviour of $h(\bar{z},\tau)$ along the straight line precisely given in the parametric form (2.7). Movements with constant velocity are realistic in the outdoor environment where the receiver is mounted in a vehicle. In this case, the Doppler rates caused by the vehicle accelerations can be neglected in comparison to the experienced Doppler shifts. In contrast to this, movements of human beings are slower but more irregular. They exhibit continuous changes in their direction and rapidity so that the model (2.7) does not apply anymore. Recently, the time-variant behaviour of the radio channel has been investigated when the receiver is assumed to perform a Brownian motion [3], [4] or a displacement generated by a stochastic model whose development relies on experimental studies of human arm movements [3]. Despite the close relationship between $h(\bar{z},\tau)$ and $h(t,\tau)$ described by (2.6), the spatial and temporal behaviour of the channel may substantially differ due to the irregularities of the trajectory $\bar{z}(t)$ [5].

Other sources than receiver displacement may cause the radio channel to become time-variant. For example, shadowing, absorption or scattering may be caused by moving vehicles in an outdoor environment or persons in an indoor environment. The resulting fast variations due to changes of the multipath interference pattern contribute to the ST fluctuations of the channel, while the variations due to shadowing can be embodied in its LT fading [5]. Time variations also arise from changing the orientation of the receiver antenna [6], due to its usually non-isotropic field pattern, and from the time fluctuations of the electrical properties of the scattering objects like fluorescent tubes [7].

The term CR is also used in the sequel to refer to $h(\bar{z},\tau)$ when the underlying discussion concerns $h(\bar{z},\tau)$ and $h(t,\tau)$ without distinction.

2.1.4 The Sources of Randomness

Radio environments may have extremely different geographical and electrical features, e.g., indoor and outdoor environments, which in turn may lead to basically different dominant propagation mechanisms. For that reason, categories of environments have been identified within which the propagation scenarios are expected to be quite similar. These categories are characterised by the cell type, i.e., macro-, micro-, and picocells, and the area type (urban, suburban, rural, etc. for macrocells). However, variability remains between the environments within a given

category, such as in the arrangement, the mean height, and the electrical properties of the buildings in an urban area, which can be conceived as a source of randomness. Moreover, the features of a specific environment in a given category usually cannot be entirely described. Especially, the geometrical and electrical properties of the objects interacting with the electromagnetic field can only be specified up to a certain level of accuracy. This indeterminateness can also be viewed as an additional cause of randomness. A third source of randomness is the indeterminateness with regard to the specification of the receiver position or of the factors leading to time variations. Even receiver movements with constant velocity are usually not completely described. The velocity is usually specified but not the starting point or even the direction of the motion. The three sources above contribute to make the FDDSF and therefore the CRs random.

2.1.5 Characterisation of the Small-Scale/Short-Term Fluctuations

Model Assumptions. The following assumption is made to describe the behaviour of the FDDSF and the CRs over small areas.

Assumption II: Uniform unattenuated plane waves are impinging in a neighbourhood of the receiver position.

Let O denote an arbitrary local reference point in this area (see Fig. 2.1). The location of O with respect to O_{ref} and the receiver position with respect to O are described by the vectors $\bar{z}_o$ and $\dot{x}$, respectively. Then, the FDDSF can be written as

$$E(\dot{x},\Omega,\tau) = \exp\left\{ j2\pi\lambda^{-1}\left\langle \dot{a}_r(\Omega)\,\middle|\,\dot{x}\right\rangle\right\} E\left(\Omega,\tau + c^{-1}\left\langle \dot{a}_r(\Omega)|\dot{x}\right\rangle\right), \quad (2.8)$$

where $E(\Omega,\tau)$ is the FDDSF at O, i.e., $E(\Omega,\tau) := E(\bar{z}_0,\Omega,\tau)$, $\langle\cdot|\cdot\rangle$ is the scalar product, λ and c denote the wavelength and the velocity of light, respectively. The terms $2\pi\lambda^{-1}\left\langle \dot{a}_r(\Omega)|\,\dot{x}\right\rangle$ and $c^{-1}\left\langle \dot{a}_r(\Omega)|\,\dot{x}\right\rangle$ in (2.8) describe the spatial dependency of the phase and the delay, respectively, of the impinging waves. With (2.8) the CIR $h(\bar{x},\tau)$ becomes

$$h(\dot{x},\tau) = C\int \exp\left\{ j2\pi\lambda^{-1}\left\langle \dot{a}_r(\Omega)\,\middle|\,\dot{x}\right\rangle\right\} f(\Omega)^T E\left(\Omega,\tau + c^{-1}\left\langle \dot{a}_r(\Omega)|\dot{x}\right\rangle\right) d\Omega. \quad (2.9)$$

Assumption III: The term $c^{-1}\left\langle \dot{a}_r(\Omega)\,\middle|\,\dot{x}\right\rangle$ in (2.9) is discarded.

Hence, the variation of the propagation delays due to the modification of the propagation path lengths is neglected. This assumption is realistic provided that the

receiver position is not too far from O in the sense that the product of $\|\vec{x}\|$ times the signal bandwidth is much smaller than c. Under Assumption III, $E(\vec{x},\Omega,\tau)$, $h(\vec{x},\tau)$, and $h(t,\tau)$ simplify to

$$E(\vec{x},\Omega,\tau) = \exp\left\{ j2\pi\lambda^{-1}\left\langle \vec{d}_r(\Omega)|\vec{x}\right\rangle\right\}E(\Omega,\tau), \tag{2.10}$$

$$h(\vec{x},\tau) = C\int \exp\left\{ j2\pi\lambda^{-1}\left\langle \vec{d}_r(\Omega)|\vec{x}\right\rangle\right\} f(\Omega)^T E(\Omega,\tau)d\Omega, \tag{2.11}$$

$$h(t,\tau) = C\int \exp\left\{ j2\pi\lambda^{-1}\left\langle \vec{d}_r(\Omega)|\vec{x}(t)\right\rangle\right\} f(\Omega)^T E(\Omega,\tau)d\Omega,$$

respectively.

WSSUS Property

Assumption IV: The FDDSF at O is a realisation of an orthogonal stochastic measure or using Bello's terminology [8] of an uncorrelated process in (Ω,τ).

Assumption IV is a mathematical formulation of the fact that the electric fields of waves impinging from different directions or exhibiting different delays are uncorrelated. Using Bello's formalism, this statement reads

$$\mathrm{E}\left[E(\Omega,\tau)^* E(\Omega',\tau')^T\right] = \mathrm{E}\left[E(\Omega,\tau)^* E(\Omega,\tau)^T\right]\delta(\Omega'-\Omega)\,\delta(\tau'-\tau) \tag{2.12}$$

In the above expression $\mathrm{E}[\cdot]$ and $[\cdot]^*$ denote the expectation and the complex conjugation, respectively. The form of the right-hand side in (2.12) suggests that $E(\Omega,\tau)$ and $E(\Omega',\tau')$ are uncorrelated unless $(\Omega',\tau')=(\Omega,\tau)$. Bello's formalism may lead to inconsistencies such as for example when one tries to evaluate both sides in (2.12) for $(\Omega',\tau')=(\Omega,\tau)$. These difficulties arise because $E(\Omega,\tau)$ is not a regular process. A rigorous mathematical approach consists of regarding $E(\Omega,\tau)$ as a generalised process, i.e., as a random distribution over an appropriate space of test functions defined on the (Ω,τ)-space. However, working within the framework of distribution theory requires a high mathematical background, especially to avoid the pitfalls arising from the use of the above formalism. An alternative, more accessible mathematical framework exists within which $E(\Omega,\tau)$ is conceived as a stochastic measure [9], [10], [3]. The latter assigns a number to any not "too wild" subset of the (Ω,τ)-space in the same way as does for example a probability measure. A stochastic measure differs from a measure by the fact that the assigned number is not deterministic but random. Within this framework, (2.12) states that the stochastic measure $E(\Omega,\tau)$ is orthogonal and that the term denoted by

$\mathrm{E}\left[E(\Omega,\tau)^{*}E(\Omega,\tau)^{T}\right]$ is its structure matrix [9]. In the sequel, the notation by Bello will be retained despite its shortcomings to make the treatment more accessible. However, all the derived results reported here using Bello's formalism have been checked to have a mathematically rigorous counterpart within the linear theory of random processes [9]. The matrix

$$F(\Omega,\tau):=\mathrm{E}\left[E(\Omega,\tau)^{*}E(\Omega,\tau)^{T}\right]=\begin{bmatrix}\mathrm{E}\left[\left|E_h(\Omega,\tau)\right|^2\right] & \mathrm{E}\left[E_h(\Omega,\tau)^{*}E_v(\Omega,\tau)\right]\\ \mathrm{E}\left[E_v(\Omega,\tau)^{*}E_h(\Omega,\tau)\right] & \mathrm{E}\left[\left|E_v(\Omega,\tau)\right|^2\right]\end{bmatrix}$$

can be referred to as the wideband coherence matrix of the electric field in the sense of [11] or in Bello's terminology as the field direction-delay-scattering matrix at location O.

From (2.10) and (2.12) it follows that

$$\mathrm{E}\left[E(\bar{x},\Omega,\tau)^{*}E(\bar{x}+\bar{\Delta}x,\Omega',\tau')^{T}\right]=\exp\left\{j2\pi\lambda^{-1}\left\langle\bar{a}_r(\Omega)|\bar{\Delta}x\right\rangle\right\}F(\Omega,\tau)\,\delta(\Omega'-\Omega)\,\delta(\tau'-\tau) \tag{2.13}$$

The right-hand side above depends on the location only through the lag $\Delta\dot{x}$. Thus, in addition to being uncorrelated in (Ω,τ), $E(\bar{x},\Omega,\tau)$ is also wide-sense-stationary (WSS) in $\dot{x}$. It immediately follows from (2.11) and (2.13) that the space-variant CIR is also WSS in $\dot{x}$ and uncorrelated in τ, i.e.,

$$\mathrm{E}\left[h(\dot{x},\tau)^{*}h(\dot{x}+\dot{\Delta}x,\tau')\right]=Q\left(\dot{\Delta}x,\tau\right)\delta(\tau'-\tau)$$

with

$$\begin{aligned}Q\left(\dot{\Delta}x,\tau\right):&=\mathrm{E}\left[h(\dot{x},\tau)^{*}h(\dot{x}+\dot{\Delta}x,\tau)\right]\\&=|C|^2\int\exp\left\{j2\pi\lambda^{-1}\left\langle\dot{d}_r(\Omega)|\dot{\Delta}x\right\rangle\right\}f(\Omega)^{H}F(\Omega,\tau)\,f(\Omega)d\Omega,\end{aligned} \tag{2.14}$$

where $[\cdot]^{H}$ is the Hermitian operator, i.e., $[\cdot]^{T}:=\left[[\cdot]^{*}\right]^{T}$. In Bello's terminology, $Q\left(\dot{\Delta}x,\tau\right)$ is referred to as the delay cross-power spectral density function. A more suggestive expression is wideband spatial correlation function (CF). Thus, under the assumptions stated above the radio channel is wide-sense-stationary and uncorrelated-scattering (WSSUS). The propagation environment when regarded as a "device" which generates the FDDSF also exhibits the WSSUS property.

If *Assumption III* is removed, i.e., if the location dependency of the propagation delay is taken into account, then $E(\vec{x},\Omega,\tau)$ and $h(\dot{x},\tau)$ still remain WSS but are no longer uncorrelated in (Ω,τ) and τ, respectively [4]. In this case, the propagation environment and the channel are WSS in $\dot{x}$ but not US in (Ω,τ) and τ, respectively.

Applying the same rationale as above to the time-variant CR yields

$$\mathrm{E}\left[h(t,\tau)^{*}h(t+\Delta t,\tau')\right]=\mathrm{E}\left[h(t,\tau)^{*}h(t+\Delta t,\tau)\right]\delta(\tau'-\tau) \tag{2.15}$$

with

$$\mathrm{E}\left[h(t,\tau)^{*}h(t+\Delta t,\tau)\right]=|C|^{2}\int\mathrm{E}\left[\exp\left\{j2\pi\lambda^{-1}\left\langle\dot{\vec{a}}_{r}(\Omega)|\vec{x}(t+\Delta t)-\vec{x}(t)\right\rangle\right\}\right]f(\Omega)^{H}F(\Omega,\tau)\,f(\Omega)\,d\Omega \tag{2.16}$$

The expectation in the right-hand side term is taken with respect to the random vectors $\vec{x}(t+\Delta t)$ and $\vec{x}(t)$. From (2.15), $h(t,\tau)$ is uncorrelated in τ. Furthermore, it is WSS in t if, and only if, the expectation in (2.16) does not depend on this variable. In particular, this condition holds for a receiver displacement with constant velocity (2.7). Indeed, for such a movement the expectation above reduces to

$$\mathrm{E}\left[\exp\left\{j2\pi\lambda^{-1}\left\langle\dot{\vec{a}}_{r}(\Omega)|\dot{\vec{x}}(t+\Delta t)-\dot{\vec{x}}(t)\right\rangle\right\}\right]=\exp\left\{j2\pi\lambda^{-1}\left\langle\dot{\vec{a}}_{r}(\Omega)|\dot{\vec{v}}\right\rangle\Delta t\right\}.$$

The term $\lambda^{-1}\left\langle\dot{\vec{a}}_{r}(\Omega)|\dot{\vec{v}}\right\rangle$ is the Doppler shift of a wave with incidence direction Ω. The random movements mentioned in Section 2.1.3 also lead to a time-variant CR which is WSS in t [3].

Assumption V: For the random motion considered in the sequel the expectation in (2.16) does not depend on t.

The function

$$Q(\Delta t,\tau):=\mathrm{E}\left[h(t,\tau)^{*}h(t+\Delta t,\tau)\right] \tag{2.17}$$

is called the wideband time CF of the channel.

The time-variant transfer function of the channel is the partial Fourier transform of $h(t,\tau)$ with respect to τ:

$$H(t,f):=\int\exp\{-j2\pi\tau t\}h(t,\tau)\,d\tau\,. \tag{2.18}$$

The fact that $h(t,\tau)$ is WSS in t and uncorrelated in τ implies that $H(t,f)$ is WSS, and conversely. The autocorrelation function (ACF) of $H(t,f)$

$$R(\Delta t, \Delta f) := \mathrm{E}\left[H(t, f)^{*} H(t+\Delta t, t+\Delta f)\right] \tag{2.19}$$

is the time-frequency CF of the channel. According to the Bochner-Khinchin Theorem [9,Theorem 2, p. 208] there exists a uniquely defined measure $P(\tau, \nu)$ such that

$$R(\Delta t, \Delta f) = \int\int \exp\{j2\pi(\nu\Delta t - \tau\Delta f)\} P(\tau, \nu) d\tau d\nu . \tag{2.20}$$

The measure $P(\tau, \nu)$ is called the delay-Doppler-scattering function of the channel. The wideband CF is related to $R(\Delta t, \Delta f)$ and $P(\tau, \nu)$ according to

$$R(\Delta t, \Delta f) = \int \exp\{-j2\pi\tau\Delta f\} Q(\Delta t, \tau) d\tau \tag{2.21}$$

and

$$Q(\Delta t, \tau) = \int \exp\{j2\pi\nu\Delta t\} P(\tau, \nu) d\nu , \tag{2.22}$$

respectively. In the above discussion, attention is intentionally focused exclusively on the characterising functions of WSSUS systems which have been the object of experimental investigations in the COST 231 action. A comprehensive treatment of the characterisation of linear time-variant systems is given in [8].

Time Dispersion and Frequency Selectivity. Setting $\bar{\Delta}x = 0$ in (2.14) or $\Delta t = 0$ in (2.17) yields the delay-scattering function or power delay profile of the channel:

$$\begin{aligned} P(\tau) &:= \mathrm{E}\left[\left|h(\dot{x}, \tau)\right|^2\right] = Q(\dot{\Delta}x, \tau)\Big|_{\bar{\Delta}x=0} \\ &= \mathrm{E}\left[\left|h(t, \tau)\right|^2\right] = Q(\Delta t, \tau)\Big|_{\Delta t=0} . \end{aligned} \tag{2.23}$$

From (2.14) and (2.22), $P(\tau)$ can also be obtained as

$$P(\tau) = |C|^2 \int f(\Omega)^H F(\Omega, \tau) f(\Omega) d\Omega = \int P(\tau, \nu) d\nu .$$

For theoretical investigation and simulation purposes, $P(\tau)$ is frequently assumed to behave according to

$$P(\tau) = \frac{P}{\sigma_\tau} \exp\left\{-\frac{\tau}{\sigma_\tau}\right\}, \tag{2.24}$$

where P is the mean received power

$$P := |C|^2 \int\int f(\Omega)^H F(\Omega,\tau)\, f(\Omega) d\tau d\Omega = \int P(\tau) d\tau = \int\int P(\tau,\nu) d\tau d\nu \tag{2.25}$$

and σ_τ denotes the delay spread subsequently defined. The adequacy of this choice is questioned in [12] considering that the power decays as a function of the distance according to a power law with an exponent which typically takes a value in the range 2 to 5 (see Chapter 4). The power delay profile has been theoretically investigated considering a conceptual situation where scatterers are independently and uniformly distributed in space and the same power decay exponent is used for each propagation path. In this model, the tail of the power delay profile asymptotically obeys a power law. Estimated delay scattering functions obtained from measurements in rural areas exhibit a similar behaviour with a power decay exponent equal to 3.5.

The instantaneous delay spread which is defined as

$$(\sigma_\tau)_{\mathrm{i}}(\dot{x}) := \sqrt{\frac{1}{P_{\mathrm{i}}(\dot{x})} \int \left[\tau - (\mu_\tau)_{\mathrm{i}}(\dot{x})\right]^2 \left|h(\dot{x},\tau)\right|^2 d\tau}$$

provides a measure of the width of $h(\dot{x},\tau)$. In the expression above, $P_{\mathrm{i}}(\dot{x})$ is the instantaneous received power

$$P_{\mathrm{i}}(\dot{x}) := \int \left|h(\dot{x},\tau)\right|^2 d\tau \tag{2.26}$$

and the instantaneous mean delay $(\mu_\tau)_{\mathrm{i}}(\dot{x})$ is the centre of gravity of $\left|h(\dot{x},\tau)\right|^2$:

$$(\mu_\tau)_{\mathrm{i}}(\dot{x}) := \frac{1}{P_{\mathrm{i}}(\dot{x})} \int \tau \left|h(\dot{x},\tau)\right|^2 d\tau \,.$$

The delay spread is defined as

$$\sigma_\tau := \sqrt{\frac{1}{P} \int \left[\tau - \mu_\tau\right]^2 P(\tau) d\tau} \,. \tag{2.27}$$

This quantity gives a measure of the width of the delay-scattering function $P(\tau)$. In (2.27), μ_τ is the mean delay defined as

$$\mu_\tau := \frac{1}{P} \int \tau P(\tau) d\tau \,. \tag{2.28}$$

Theoretical investigations [14] have shown that the delay spread σ_τ and the expectation of the instantaneous delay spread $\mathrm{E}\left[(\sigma_\tau)_{\mathrm{i}}(\dot{x})\right]$ may be quite different for

the Gaussian two-path channel. Here, the expectation is with respect to the random process $h(\dot{x},\tau)$. Simulations indicate that this difference decreases towards 0 as the number of components in the CIR increases.

The delay spread is not an appropriate dispersion parameter for assessing the performance of modems with finite equaliser depth since it does not directly relate to the delay window which the equaliser is capable to cope with. For this reason [13, 30] proposed the following two more suitable parameters. The interference ratio Q_D is defined as the maximum ratio (in dB) between the power inside and that outside a delay interval of a fixed length D:

$$Q_D := 10\log\left(\max\left\{\frac{\int_W P(\tau)d\tau}{P-\int_W P(\tau)d\tau} : W = \text{delay interval of leng } D\right\}\right).$$

The delay window W_q is the minimum delay interval such that the ratio between the power inside and outside it equals a fixed ratio q (in dB):

$$W_q := \min\left\{W = \text{delay interval} : 10\log\left(\frac{\int_W P(\tau)d\tau}{P-\int_W P(\tau)d\tau}\right) = q\right\}.$$

For GSM, q and D are chosen to be 9dB and 16μs corresponding to the tolerable interference level and delay window. It has been confirmed in [60] and [61] that these parameters predict link performance better than the delay spread.

Time-dispersion causes frequency selectivity, i.e., fluctuations of the amplitude of $H(t,f)$ when f changes. The frequency CF of the channel is defined to be

$$R(\Delta f) := \mathrm{E}\left[H(t,f)^* H(t,f+\Delta f)\right] = R(\Delta t,\Delta f)\big|_{\Delta t=0}.$$

According to (2.19) and (2.22), the following identities hold:

$$R(\Delta f) = \int \exp\{-j2\pi\tau\Delta f\}P(\tau)d\tau\,.$$

The coherence bandwidth is a quantity which describes the width of the main lobe of the absolute value of the frequency CF. It is defined for a given coherence level $\rho \in [0,1]$ as

$$B_\rho := \begin{cases} \arg\min\left\{ \Delta f \geq 0 : \frac{1}{P}\left|R(\Delta f)\right| < \rho \right\} & ;\ \rho \in (0,1] \\ \lim_{\rho \to o} B_\rho & ;\ \rho = 0 \end{cases}. \tag{2.29}$$

An uncertainty relation exists between the delay spread and the coherence bandwidth [15] stating that the product of these quantities is lower-bounded according to

$$\sigma_\tau B_\rho \geq \frac{1}{2\pi}\arccos(\rho). \tag{2.30}$$

Moreover, the lower bound is attained if, and only if, the delay-scattering function is of the form $P(\tau) = \frac{P}{2}\left[\delta(\tau - \tau_1) + \delta(\tau - \tau_2)\right]$, in which case $\sigma_\tau = \left|\tau_2 - \tau_1\right| / 2$.

The average link quality of a non-equalised system like DECT is closely related to the average delay spread, whereas the instantaneous delay spread does not characterise the instantaneous (burst) link performance of such a system. Indeed, the latter parameter does not provide any information about the actual position of the fades in the frequency domain. In [116] it has been found that the link quality depends on whether an instantaneous fade is present in the system bandwidth B_S or not. This observation has motivated the introduction of the frequency magnitude variation parameter [116] which is defined as

$$V_{B_S} := \frac{\max\left\{\left|H(f)\right| : f \in B_S\right\}}{\min\left\{\left|H(f)\right| : f \in B_S\right\}}.$$

The advantage of this frequency domain parameter is that it can be determined using only the actual system bandwidth.

Doppler Dispersion and Time Selectivity. The Doppler-scattering function or power Doppler profile and the time CF of the channel are defined to be

$$P(\nu) := \int P(\tau, \nu)\, d\tau \tag{2.31}$$

and

$$R(\Delta t) := \mathrm{E}\left[H(t, f)^* H(t + \Delta t, f)\right] = R(\Delta t, \Delta f)\big|_{\Delta f = 0}, \tag{2.32}$$

respectively. It follows from (2.20) that

$$R(\Delta t) = \int \exp\{j 2\pi \nu \Delta t\} P(\nu)\, d\nu.$$

Let us assume that the receiver is moving with constant velocity (see (2.7)) and that the radiating sources are randomly selected in the following way: (1) the locations are independently and uniformly distributed in space, (2) the radiated powers are independently and identically distributed with finite expectation, and (3) the locations and the radiated powers are independent random variables. Then, $P(\nu)$ coincides with the well-known Clarke's spectrum [16]

$$P(\nu) = \begin{cases} \dfrac{P}{\pi\sqrt{\nu_D^2 - \nu^2}}; |\nu| < \nu_D \\ 0 \qquad\qquad ; \text{otherwise} \end{cases}, \tag{2.33}$$

where $\nu_D := \|\dot{v}\| / \lambda$ is the maximal Doppler shift. The power Doppler profiles which are obtained experimentally in a specific environment usually have a shape different from (2.33). The reason is that the assumptions stated above are rarely satisfied. Actually, the Clarke's spectrum has to be regarded as an average power Doppler profile over many environments considering a fixed velocity magnitude $\|\bar{v}\|$. As postulated in [5] and shown in [3] (see also Section 4.7.4), when the receiver performs irregular movements in a random manner, then the resulting power Doppler profiles are basically different from those arising due to movements with constant velocity.

The mean average Doppler shift μ_ν, the Doppler spread σ_ν, and the coherence time T_ρ are defined by replacing the delay-scattering function and the frequency CF by the Doppler-scattering function and the time CF, respectively, in the defining equations (2.28), (2.27), and (2.29). An uncertainty relation similar to (2.30) also exists between σ_ν and T_ρ.

Discrete Channel Model. This model relies on the assumption that the FDDSF and therefore the space-variant CIR only embrace the coherent part in (2.1) and (2.4), respectively. Provided that Assumptions I and II hold,

$$\begin{aligned} E(\bar{x},\Omega,\tau) &= E_c(\bar{x},\Omega,\tau) \\ &= \sum_{j=1}^{J} E_j \exp\left\{ j2\pi\lambda^{-1}\left\langle \bar{a}_r(\Omega_j) \middle| \bar{x} \right\rangle \right\} \delta(\Omega - \Omega_j)\, \delta\left(\tau - \left(\tau_j - c^{-1}\left\langle \bar{a}_r(\Omega_j) \middle| \bar{x} \right\rangle\right)\right) \\ h(\dot{x},\tau) &= h_c(\dot{x},\tau) \\ &= \sum_{j=1}^{J} h_j \exp\left\{ j2\pi\lambda^{-1}\left\langle \dot{a}_r(\Omega_j) \middle| \dot{x} \right\rangle \right\} \delta\left(\tau - \left(\tau_j - c^{-1}\left\langle \dot{a}_r(\Omega_j) \middle| \dot{x} \right\rangle\right)\right) \end{aligned}$$

with $h_j := C\, f(\Omega_j)^T E_j$, so that the time-variant CR reads in this case

$$h(t,\tau)=\sum_{j=1}^{J}h_j\exp\left\{j2\pi\lambda^{-1}\left\langle \dot{d}_r(\Omega_j)\middle|\dot{x}(t)\right\rangle\right\}\delta\left(\tau-\left(\tau_j-c^{-1}\left\langle \dot{d}_r(\Omega_j)\middle|\dot{x}(t)\right\rangle\right)\right)$$

Under Assumption III, the three sums above simplify to

$$E(\dot{x},\Omega,\tau)=\sum_{j=1}^{J}E_j\exp\left\{j2\pi\lambda^{-1}\left\langle \dot{d}_r(\Omega_j)\middle|\dot{x}\right\rangle\right\}\delta(\Omega-\Omega_j)\,\delta(\tau-\tau_j),$$

$$h(\dot{x},\tau)=\sum_{j=1}^{J}h_j\exp\left\{j2\pi\lambda^{-1}\left\langle \dot{d}_r(\Omega_j)\middle|\dot{x}\right\rangle\right\}\delta(\tau-\tau_j),$$

$$h(t,\tau)=\sum_{j=1}^{J}h_j\exp\left\{j2\pi\lambda^{-1}\left\langle \dot{d}_r(\Omega_j)\middle|\dot{x}(t)\right\rangle\right\}\delta(\tau-\tau_j).$$

A sufficient condition for the WSSUS property to be satisfied, i.e., for Assumption IV to hold, is that the waves' parameters $\{\Omega_j,\tau_j,E_j\}$ are randomly selected in such a way that the field vectors $\{E_j\}$ are uncorrelated with zero mean and finite covariance and, moreover, are independent of the incident characteristics $\{\Omega_j,\tau_j\}$.

2.1.6 Characterisation of the Large-Scale Fluctuations of the Channel

Path Loss and Shadowing Effects. Computing the average of $P_{\mathrm{i}}(\dot{z})$ in (2.26) over a small domain $A(\bar{z})$ around $\dot{z}$ to cancel out the SS fluctuations yields the averaged received power

$$\langle P\rangle(\dot{z}):=\frac{1}{\mathrm{Vol}[A(\dot{z})]}\int_{A(\bar{z})}P_{\mathrm{i}}(\dot{y})d\dot{y}, \tag{2.34}$$

with $\mathrm{Vol}[A]$ denoting the volume of the domain A. This average can also be computed considering a surface or a line rather than a volume. Let $h_{A(\bar{z})}(\dot{x},\tau)$ denote the SS characterisation of the space-variant CIR over $A(\bar{z})$ as presented in Section 2.1.5. According to (2.25) the mean received power is given as

$$P(\dot{z}):=\mathrm{E}\left[\int\left|h_{A(\bar{z})}(\dot{x},\tau)\right|^2d\tau\right]=\int P_{A(\bar{z})}(\tau)d\tau\,.$$

If the assumptions made in Sections 2.1.5 are realistic over $A(\bar{z})$, then $\langle P\rangle(\bar{z})$ is close to $P(\bar{z})$. The ratio $\langle P\rangle(\dot{z}) / P_T$ expressed in dB is decomposed into the sum

$$-\left[\langle P\rangle(\dot{z}) / P_T\right]\Big|_{\mathrm{dB}} = L(\dot{z}) + \Delta L(\dot{z}), \tag{2.35}$$

where $L(\bar{z})$ is the path loss and $\Delta L(\bar{z})$ describes the fluctuations of the averaged received power around $L(\bar{z})$ which result from shadowing effects. Prediction models for $L(\bar{z})$ are presented in Chapter 4. Usually, $\Delta L(\bar{z})$ is assumed to be a realisation of a Gaussian process entirely specified by its ACF.

Transitions Between Areas with Different Propagation Configurations. The space-variant CIR corresponding to a transition from an area A to another one A' (see Fig. 2.1) with possibly different propagation configurations, such as encountered in a transition from a LOS to a NLOS situation, can be built up from the SS characterisation of the CIRs over A and A' according to

$$h_{A\to A'}(\dot{x},\tau) := \left(1-b(\dot{x})\right)h_A(\dot{x},\tau) + b(\dot{x})h_{A'}\left(\dot{x}-\dot{x}_o,\tau\right).$$

Here, $b(\bar{x})$ is a smooth unit step function which increases from 0 to 1 over the transition domain from A to A'. Situations where specific components $h_\nu(\dot{x},\tau)$ of the CIR (see (2.5)) vanish or appear can be handled in the same way as above by multiplying them either with $\left(1-b_\nu(\dot{x})\right)$ or $b_\nu(\dot{x})$ where $b_\nu(\dot{x})$ is a function similar to $b(\bar{x})$.

Fluctuations of the Propagation Delays. As the receiver moves over large areas, the propagation paths change so that the components $E_\nu(\dot{z},\Omega,\tau)$ and $h_\nu(\dot{z},\tau)$ of the FDDSF (see (2.3)) and the space-variant CIR (see (2.5)), respectively, drift on the τ-axis as $\dot{z}$ varies. One way to account for this effect consists of removing Assumption III and computing the FDDSF and the CIR from (2.8) and (2.9), respectively.

Fluctuations of the Incidence Directions. As the receiver location changes over wide areas, the direction of the radiating sources with respect to its position varies. As a consequence, the components $E_\nu(\dot{z},\Omega,\tau)$ of the FDDSF (see (2.3)) move in the Ω-space. Assumption II does not allow to account for this effect. Modifications of the incidence direction as a function of the position can be taken into account by assuming that spherical rather than plane waves are impinging in a neighbourhood of the receiver. Hitherto, no publication seems to be available which addresses this issue.

2.2 Measurement Techniques - Channel Sounders

Jean-Claude Bic, CNET, France Telecom, France

The first step to characterise the radio mobile channel is to obtain reliable measurements. The quality of the prediction models depends crucially on the measured data. COST 231 is aimed at the third generation of digital cellular systems which will occupy a larger bandwidth either in TDMA or CDMA access than the current systems and will be operated in various environments. As a consequence the investigation of propagation needs channel sounders able to measure the variability and frequency selective behaviour of the channel by means of either the Impulse Response (IR) or the transfer function in at least the system bandwidth. The sounder will also have to cope with different constraints according to the environment, maximum excess delay, time resolution, etc., and must demonstrate a sufficient flexibility. Of course, field strength measurements are still needed for path-loss modelling and planning purposes but the techniques are rather well-known and the following sections will be focused on the wideband measurements techniques. Since the beginning of the COST 231 project, measurements have been carried out with many channel sounders. They have been designed according to different techniques but they could be classified in three main categories: pulse sounding, time domain (pulse compression) and frequency domain techniques.

The main performance of a sounder is given by:

- the maximum duration of the measured IR for delay range;
- the bandwidth or equivalently the time resolution to discriminate between two echoes;
- the dynamic range to detect an echo out of the noise level;
- the acquisition rate to measure successive IRs for Doppler analysis;

Measurements of the Direction of Arrival are also a new feature which is important to validate prediction methods based on ray tracing and different devices have been added to sounders, in order to perform this kind of [17-21].

2.2.1 Pulse sounders

They are very simple to implement and give a good resolution but they suffer from the need of high peak-to-mean power ratio. Several of them have been implemented mostly for indoor measurements where high transmitted power is not critical:

- the pulse sounder of the Aalborg University [22] with a pulse width of 100 ns performs measurements in office buildings;
- the pulse sounder [23, 24] operated by VTT has a pulse-width of about 8 ns and a dynamic range of 25 dB;
- the pulse sounder of Telecom Denmark [25] with a 80-ns resolution has been used in indoor office, shopping centre and railway station;
- the pulse sounder [26, 27] of DeTeMobil used in picocell and microcell measurements for DECT has a dynamic range less than 20 dB;
- the pulse sounder developed by Telefonica [28] with pulse width range from 40 to 200 ns and repetition rate from 1 to 100 μs.

2.2.2 Time domain sounders

The main characteristics of the pulse compression channel sounders that contributed to COST 231 are given in Table 2.1. Several "classical" channel sounders based on PN sequences at the transmitter and sliding correlation at the receiver either by analogue or digital means have been widely used for IR measurements especially within the framework of second generation systems like GSM and DECT. They have good performances in terms of resolution but relatively poor in terms of maximum acquisition rate and they provide only the amplitude of the IR.

- the Swiss-PTT RCS-900 (Real-time Channel Sounder) [29,30] SAW correlator with a 3 MHz 3-dB bandwidth has been used for measurements in Texas in high-rise buildings environment [31]; a new device called Universal Channel Analyser [32] has been developed incorporating the sounders RCS-900 and RCS-1900 and offers real-time analyses in addition to measurements;
- the Bellcore sounder [33] with a 25 MHz 3 dB-bandwidth is based on the sliding correlator approach has been operated indoor measurements where Doppler effects are not so important. It has also be used by Aalborg University to investigate polarisation diversity [34] and antenna diversity after some improvements [35];
- the BT sounder [36] has a time resolution of 50 ns and delays up to 12.75 ms with a dynamic range of about 31 dB, but limited to 4 IR/s;

- the Lund University sounder [37] is derived from the sliding correlator approach by direct conversion at the receiver to obtain a high resolution of 10 ns. A cable is used between the transmitter and the receiver for indoor measurements.

Tables 2.1 Characteristics of pulse compression channel sounders contributed to COST 231

Country	Austria	Denmark	France	Germany	Germany
Institution	University of Wien	University of Aalborg	CNET	DBP Telekom University of Erlangen	DBP Telekom University of Erlangen
Equipment	DCCS 1800			RUSK 400	RUSK 5000
Frequency range (MHz)	1800	980	900, 2200	890..960	50..1000
Bandwidth (MHz)	15		12.5/25/50	0.4	5.75
peak output power (W)	1	10			
excitation	PNS	PNS	PNS	mod. PNS	mod. PNS
Sequence length (symbols)	7.. 1023	511	127, 255, 511	127	1023
Chiprate (Msymbol/s)	30	50	15	1	10
Modulation	BPSK	BPSK	BPSK	DSB-AM	VSB-AM
Max. duration of IR (us)	34	51	34	127	102.3
Time resolution of IR (us)	0.05	0.02	0.067	3.5	0.24
Max. Acquisition rate (IR/S)	8	> 20	800	44	42 (208)**
Total dynamic range (dB)	>80	100			
Instant. dyn. range (dB)	>28	> 40	>30	>35	>30
Sensitivity (dBm)	-101			-110	-100
Correlation technique	digital correlation	sliding correlation (digital)	Postprocess. inverse filtering	unbiased ML estimation via cyclic inverse filter	unbiased ML estimation via cyclic inverse filter
COST 231 TD Nr. (yy)-nn	93-88	93-08	90-31	90-40/41/75	92-09

Country	Germany	Germany	Ireland	Italy	Norway
Institution	MEDAV	Siemens	Trinity College	CSELT	Telenor R&D
Equipment	RUSK X				
Frequency range (MHz)	900..1800	870-980 1805-1880	980, 1808	2000	900 and 1700
Bandwidth (MHz)	0.1.- 6.0	5, 10, 20	10	100	1, 2, 4, 8
peak output power (W)			35 (average)	0.3	20
Excitation	Chirp	Digital signal (low crest factor)	PNS/Chirp	PNS	Chirp
Sequence length (symbols)	128, 256, 512, 1024	BT = 256, 512, 1024	*	511, 2047	128
Chiprate (Msymbol/s)	10		*BT=256	50 MHz	
Modulation	DSB-AM	DSB-AM	*Vector mod.	BPSK	(leave open)
Max. duration of IR (us)	102.4	102.4	25.6	10.6 - 41.3	16 - 128
Time resolution of IR (us)	0.23		0.1	0.02	0.125 - 1
Max. Acquisition rate (IR/S)	39 (390)**	1000	1000	> 4000	15
Total dynamic range (dB)		100	--	60 (adjust.)	> 80
Instant. Dyn. range (dB)	>35	40	50	> 30	> 30
Sensitivity (dBm)	-115		-115	-92	-121 -148[1]
Correlation technique	unbiased ML estimation via cyclic inverse filter	unbiased ML estimation (matched filter + sidelobe canc.)	mismatched filtering	Coherent demodulation and cross-correlation	Multiplication in frequency domain
COST 231 TD Nr. (yy)-nn	94-125	95 - 128	93-48, 94-29	94-19	92-62

Country	Norway	Spain	Switzerland	Switzerland	UK
Institution	Telenor R&D	AlcatelSESA/UPC	Swiss PTT	ETH CTL Zurich	British Telecom
Equipment			RCS 900	RCS/RCA900 /1980	
Frequency range (MHz)	1950 - 59 GHz	900, 1900	760..1000	900, 1980	1800
Bandwidth (MHz)	6.25, 12.5, 25, 50, 100, 200	100	3	1-560	50
Peak output power (W)	0.3 or 10	0.1, 1		20	
Excitation	Chirp	PNS	Barker PNS	PNS	PNS
Sequence length (symbols)	64 to 8192	127, 511, 1023	13	127, 255, 511, 1023, 2047	255
Chiprate (Msymbol/s)		50	1.66	1-120	20
Modulation	(leave open)	BPSK	BPSK	BPSK	BPSK
Max. duration of IR (us)	0.32 - 164	2.5, 10.2, 20.4	80	1-2047	12.75
Time resolution of IR (us)	0.005 - 0.16	0.04	0.6	0.008-1	0.05
Max. Acquisition rate (IR/S)	728	40, 9, 4	7	744	4
Total dynamic range (dB)	> 80	70	70	60	
Instant. dyn. range (dB)	> 30	> 25	>25	45	>31
Sensitivity (dBm)	-110 -153[2]	- 90	-102	-75	
Correlation technique	Multiplication in frequency dom.	Sliding analogue correlator	Correlation by SAW device	Analogue correlation	Sliding SAW correlation dev.
COST 231 TD Nr. (yy)-nn	95-57	95-05	89-41, 91-45	89-39,90-79, 91-89	90-83

* Vector modulation of two DDS channels, BT product is given instead of sequence length

** Burst mode of 256 Irs

1 Dependant on measurement bandwidth and number of averaged sweeps before correlation takes place

2 Dependant on measurement bandwidth, sequence length and number of averaged sweeps before correlation takes place

Moreover, the need for better performance and for a greater flexibility to characterise a large variety of environment, both indoor and outdoor, have led to the design of new time-domain sounders, as shown in Fig. 2.3.

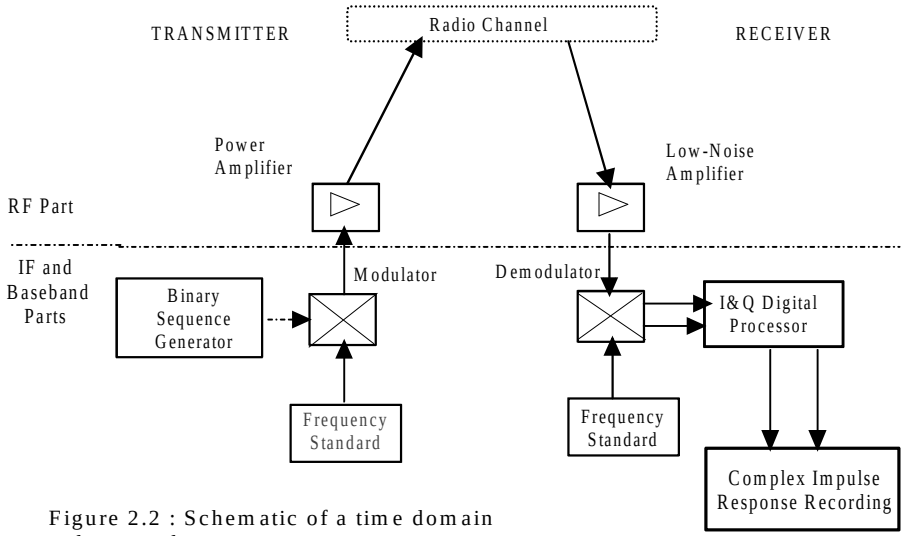

Figure 2.2 : Schematic of a time domain pulse sounder

Fig. 2.3 Schematic of a time domain pulse sounder

Most of them are based on transmitting a BPSK-modulated binary sequence periodic or not [38] having special correlation properties (PN sequence, generally). Digital processing is usually performed at the receiver, by correlation or inverse filtering of in-phase and quadrature sampled IRs and the Complex IR is obtained. The transmitter and receiver are accurately synchronised by means of very stable clocks and usually can be used both in the 900 MHz and 1.8 GHz bands. They have been widely used especially for measurements performed in RACE II projects ATDMA and CODIT [39-41]:

- RUSK "family": RUSK-5000 [41,42] designed by DBP Telekom is an improvement of the RUSK 400 built for GSM purposes [43-46]. It performs correlation of 1023-bit pseudo noise signals transmitted in a TV-bandwidth of 5.75 MHz. The digital processing give an instantaneous dynamic range better than 30 dB. RUSK X is a further extension of the former one with a carrier frequency ranging from 0.9 to 1.8 GHz and a bandwidth up to 6 MHz utilised in RACE project ATDMA [40].
- Lastly, RUSK SX [47] has been designed with respect to microcell and indoor picocells. Its resolution is 15 ns for indoor, due to a bandwidth of 120 MHz.

- The CNET sounder [41, 48-49] processes the received samples of the IR by inverse filtering to improve dynamic range and resolution and it has an adjustable 3dB-bandwidth up to 50 MHz and a sequence length up to 511 bits.
- The sounder developed at the Swiss Federal Institute of Technology [39, 50-56] and used in the RACE project 2020 CODIT has a very large bandwidth of 560 MHz, a PN-sequence up to 2043 bits and analogue correlation at the receiver. The maximum measurable Doppler shift is about 370 Hz.
- The Siemens sounder is based on the method of optimal estimation which avoided the correlation sidelobes. Especially designed test sequences guarantee measurements with low intermodulation in the transmitter amplifier [57-59].
- The CSELT sounder [39, 117], using a software receiver, performed outdoor and indoor measurements in the CODIT project in a bandwidth of 20 MHz.
- The Trinity College sounder [62] uses the mismatched filter principle to improve the noise gain of the receiver and a low-crest factor signal at the transmitter [63].
- The Direct-Conversion Channel Sounder (DCCS 1800) from Technical University of Vienna [64] has a 50 ns time resolution and a maximum excess delay of 34 µs.
- The Alcatel SESA sounder [65] was designed and built by UPC team with a 40 ns resolution to operate in indoor as well as in urban, suburban and rural environments.
- The sounder developed by Telenor R&D in 1991 [66] and the improved sounder developed in 1993 [67, 68] are based on the frequency sweep technique frequently used in radars. In the receiver a digital signal processor performs an operation corresponding to a correlation in the time domain. Although the principle is slightly different, i.e. the carrier is modulated with a bit sequence giving a frequency sweep as the output waveform, it can be considered as a pulse compression technique. It has also been used for measurements in the 60 GHz band (see Chapter 8, Section 8.4).
- The Aalborg University sounder [120] is based on a digital sliding correlator principle, allowing for programmable sweeping windows less than the PN-sequence length, thus allowing for faster acquisition rates than corresponding sliding correlators sounders. The minimum time resolution is 20 ns.

2.2.3 Frequency domain sounders

Network analysers can also be used for indoor measurements where it is possible to synchronise transmit and receive sides by means of a cable [39, 69-70]. They achieve rather easily large bandwidths (i.e., 200 MHz for the Telefonica-Ericsson analyser used in CODIT) and are more often used to characterise wideband propagation in the millimetre band than in UHF-VHF bands (see Chapter 8, Section 8.2).

2.3 Propagation measurements and their analysis

Gerhard Kadel, Deutsche Telekom, Germany

2.3.1 The need for propagation measurements

The radio propagation channel is a very important and a very critical component for mobile radio communications systems. Therefore, the detailed analysis of the radio channel is of basic importance for the design of future mobile communications systems as well as for the optimisation and extension of existing systems. Due to the complexity of the propagation phenomena and due to the statistical nature of the radio channel parameters, a reliable channel characterisation can only be based on appropriate channel measurements.

2.3.2 Objectives of the COST 231 propagation measurements

Within COST 231 a huge amount of propagation measurements were performed in the 900-MHz bands and 1800-MHz bands in a large variety of different environments ranging from pico cells and micro cells to macro cells. Different measurement techniques, which are described in the previous sections, were used. Much attention was paid to indoor investigations and to urban micro cellular investigations because these cell types will be particularly important for future UMTS systems with high capacity demands. The propagation measurements had the following objectives:

- characterisation of the channel for all types of indoor and outdoor environments relevant for current and future mobile services,
- investigation of transitions between different environments (e.g., transition between line-of-sight (LOS) and non-line-of-sight (NLOS) conditions, penetration),
- measurement of the channel conditions as function of all important factors having an influence on the channel (e.g., antenna heights, antenna patterns, base station locations, bandwidths, etc.),

- generation of data bases for (wideband) propagation modelling (software and hardware channel simulators including "stored channels"), as described in Section 2.4,
- provision of propagation data for the development, verification and optimisation of propagation prediction models as described in Chapter 4,
- investigation of performance and coverage of mobile radio systems by determination of related channel parameters out of measurements (e.g., interference ratio for GSM or delay spread for DECT) in order to determine system performance on the basis of channel characteristics [91,92],
- measurement of channel characteristic for special services (e.g., mobile services for high-speed trains).

According to the different objectives described above, different approaches for the classification of measurements were used. Measurements were categorised as function of the cell size (e.g., pico, micro, macro cells), as function of the base station visibility (LOS, NLOS), as function of terrain undulations (flat, hilly, etc.), as function of building or vegetation density, as function of the mobile speed (from stationary to high speed trains), etc..

2.3.3 Narrowband and wideband measurements

The mobile radio channel within a certain bandwidth of interest can be completely characterised by its complex time-variant impulse responses (Eq. (2.6)) or equivalently its time-variant transfer function (Eq. (2.18)). The measurement equipment must be able to record the impulse responses with a sufficient length in time and to fulfil the sampling theorem with respect to the Doppler shift (i.e. record at least two impulse responses per wavelength). For system related investigations (e.g., simulations with stored channel data) a measurement bandwidth equal to the system bandwidth is sufficient. For the development of (wideband) deterministic or statistical propagation models, a very large bandwidth for channel measurements is desirable in order to gain as much details as possible which help to understand the propagation phenomena (e.g., identification of scatterer locations) and to support the modelling approaches.

However, propagation measurements with large bandwidths produce a huge amount of data. Therefore, narrowband measurements which can be carried out and handled much simpler, are appropriate if only narrowband information is required. This is particularly the case for all types of pathloss modelling.

2.3.4 Analysis of propagation measurements

In order to generate a common platform for the analysis and exchange of propagation data, file formats are required which are equipment independent and contain all data necessary for the various methods of data analysis. Within COST 231 two file formats were used for wideband channel data: the binary "Universal Measurement File (UMF)", format developed by Technical University of Vienna and the "RACE Level2 Format" [71] which is an ASCII format developed within the RACE ATDMA project and adopted by COST 231.

Propagation measurements contain noise. Effective methods of noise reduction are required for reliable evaluation of radio channel parameters. Particularly the parameter delay spread is very sensitive for noise components at large excess delays of the impulse responses. For wideband measurements, noise thresholds, derived either from sections of measured impulse responses containing only noise or deduced from back-to-back calibration measurements, were developed to reduce the impact of noise.

From propagation measurements various channel parameters were evaluated (see Section 2.1 for definitions):

- average path loss and its short-term and long-term fluctuations,
- time variance,
- frequency selectivity,
- directions of arrivals (DOA).

In general, all channel parameters show large variations of their absolute values for different environments and rapid fluctuations.

2.3.5 Indoor measurements

Indoor propagation measurements have been carried out in the 900- and 1800-MHz range in order to develop and test the indoor propagation models presented in Chapter 4, Section 4.7. The measurements have been conducted by Alcatel Sesa, Swiss Federal Institute of Technology Zürich (ETH), Ericsson Radio Systems, France Telecom (CNET), Technical University of Catalonia (UPC), Technical University of Vienna (TUW), University of Lund and VTT Information technology. The emphasis of the research has been on office buildings which constitute the main application area of wireless indoor communication systems. Also some shopping centres and factory environments have been under study.

The indoor environments have been divided into four categories as described in Table 2.2. A small number of categories has been included in order to obtain clearly different propagation characteristics between the categories and in order to have sufficient amount of measurement data for each category. General information of the measurements carried out by the various organisations is given in Table 2.3.

Table 2.2 Indoor environment categories

Environment category	Description
Dense (D)	Environments with small rooms; typically an office where each employee has one's own room; mostly NLOS (Non-line-of-sight) conditions.
Open (O)	Environments with large rooms; typically an office where one room is shared by several employees; mostly LOS (Line-of-sight) or OLOS (Obstructed-line-of-sight) conditions.
Large (L)	Environments consisting of very large rooms; typically a factory hall, shopping centre or airport building; mostly LOS or OLOS conditions.
Corridor (C)	Transmitter and receiver along the same corridor; LOS condition

Despite of the different measurement methods and equipment, some common rules were followed in performing the measurements. The overall goal was that the measurement configuration corresponds, as much as possible, to a real communication system, involving a stationary station (base station) and a mobile station.

The base station was located on a central position in the building and the mobile station was moved into several positions within the coverage area of the base station. The base station height from floor varied between 1.5 m and 3 m. Omni-directional antennas with 1.3-2.2 dB gain were used. The transmitter power was 10 to 30 dBm. The polarisation was vertical in all of the measurements.

Averaged path loss values are required for the development of narrow-band models. These were obtained by averaging the received signal level and then calculating the path loss from Eq. (2.34). An example of measured path loss within an office building is shown in Figure 2.4.

Table 2.3 Description of indoor measurement data (NB=narrow-band, WB=wide-band)

Organisation	Frequency band(MHz)	Categ.	Numb. of meas. NB	WB	Data and building description
Alcatel [72]	1900	DC	871[1)]		2 office buildings, meas. in several floors.
ETH [80]	900	OCL		40000[3)]	subway station, airport, large office, factory
Ericsson [73]	900	DOL	100-500 [6)]		4 office buildings, airport, convention centre, casino, hospital, underground, parking garage
CNET [74]	900 900 1800	D D D	- 548 [1)] 548 [1)]		Office building without furniture in six floors Office building
Lund [75]	1800	DOL	735000 [2)]	3397 [3)]	Office building(NB&WB), shopping centre (NB) and exhibition centre (NB)
TUW [76]	1800	DOC	229[5)]	36[4)]	Office building
UPC [77]	900 1800	DLC DLC	400[1)]	35[4)]	2 office buildings
VTT [78]	900 1800	DOL DOL	325[1)] 488[1)]	82[4)]	8 office buildings (NB), 2 office buildings (NB&WB), underground hall (NB&WB), factory hall (NB)

[1)] Number of averaged measurement points
[2)] Number of samples

[3)] Number of instantaneous power delay profiles (PDPs)

[4)] Number of averaged PDPs

[5)] Number of 1-30 m long measurement routes

[6)] Number of measurement loops in each building

The used number of samples was 10 to 50 and the averaging length was 1-6 wavelengths in most of the measurements. In Ericsson's measurements the averaging was performed along a loop covering typically a small room. The considerably shorter averaging length compared to outdoor measurements is appropriate because of the high variability of the indoor environment.

The wide-band results given in Chapter 4, Section 4.7 are expressed in terms of average delay spreads in different environments. These values were obtained by averaging over all the individual measurements of each environment category.

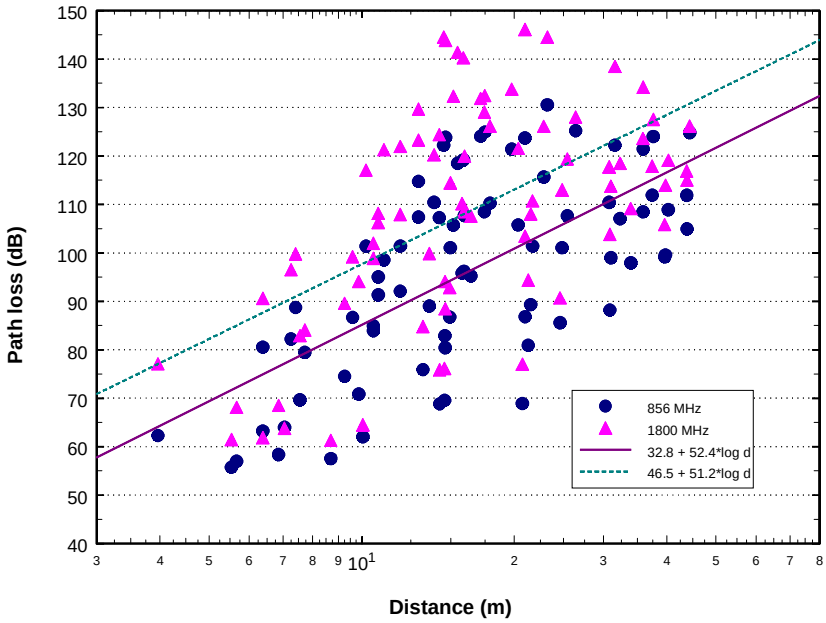

Fig. 2.4 Measured path loss as a function of distance between transmitter and receiver in a typical office building. Receiver has been in the 4th floor and transmitter has been moved to measurement points in floors 0-4.

The delay spread was calculated from the measured power delay profile (PDP) (Eq. (2.23) by using Eq. (2.27). The PDP was measured in time-domain either by using a spread-spectrum channel sounder [76,79-80] or using pulse techniques [78]. Frequency domain measurements by a network analyser and a Fourier transform were used in [81] to obtain the PDP.

Wideband polarisation state behaviour of the radio channel has been investigated in [121] at 1800 MHz. The conclusion is that the radio channel has chaotic polarisation behaviours both in the spatial and temporal domain. Average XP (cross-polarisation figures) have been found to 8.7 and 4 dB, outdoors and indoors, respectively.

Also indoor measurements aiming for the determination of directions-of-arrival (DOAs) were carried out. In [82] a measurement concept based on coherent wide band measurement in time domain was presented. The DOAs of dominant signal components at subsequent time slots were calculated by using the Maximum

Likelihood optimisation. Alternative DOA algorithms are presented in [83]. In [84] narrow-band measurements and a synthetic aperture technique are used. The DOA distribution was solved either by using normal beam forming methods or the high resolution MUSIC (Multiple Signal Classification) method.

2.3.6 Outdoor measurements

For the outdoor propagation measurements performed in the framework of COST 231 special emphasis was dedicated to path loss and frequency selectivity. For wideband UMTS systems aiming for high data rates, the frequency selectivity in outdoor environments will have a major impact on system performance.

Measurement example. In Fig. 2.5 a typical result from a wideband outdoor measurement run in a micro cellular environment is given [96]. The shape of the PDPs are plotted along a run of 300 m. Each line in the three dimensional plot represents an average over 3 m. In the first part of the run there was LOS between transmitter and receiver, in the second part there was NLOS due to shadowing from buildings. The transmitter height was 11 m, the receiver antenna height was 2 m. The average distance between transmitter and receiver was about 200 m.

2.3.7 Fading and path loss characteristics

From narrowband and wideband measurements the short term and long term fluctuations of the received power were evaluated. For the determination of the long-term fading the fast fluctuations were eliminated by averaging over a gliding window having a length of 10 to 50 wavelength. The average path loss is ranging from about 50 dB for micro cells with short LOS paths up to about 150 dB for the edges of large macro cells. It depends mainly on the distance between transmitter and receiver, the building density and the heights of base station and mobile station antennas. Guiding effects in micro cellular street canyons with LOS may result in path loss values which are up to 4 dB lower compared to free space propagation if both the transmitter and receiver antenna are well below the roof tops of the surrounding buildings [89]. In general, the path loss is increasing by 25 dB to 30 dB while moving from micro cells with LOS to micro cells with NLOS conditions [94,96].

The increase of path loss with distance varies generally between 20 dB per decade for free space conditions and may exceed 50 dB per decade for NLOS situations with very high building densities. The path loss values are in the order of 6 to 10 dB larger for the 1800-MHz range than for the 900-MHz range [122]. The time variance of the fast fading depends mainly on the carrier frequency and on the speed of the mobile. It can be described for narrowband measurements by the power Doppler profile according to Eq. (2.31) and for wideband measurements by the delay-Doppler scattering function according to Eq. (2.20). The statistical distribution of the short-term fluctuations depend on the existence of dominant propagation paths and on the measurement bandwidth with respect to the coherence bandwidth of the channel (Eq. (2.29)).

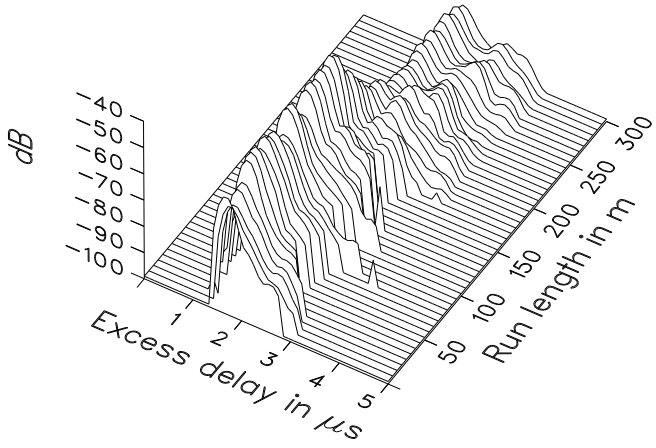

Fig. 2.5 Impulse responses along a run of 300 m in a micro cellular environment

For narrowband transmission, LOS conditions are resulting in Rice fading instead of Rayleigh fading for NLOS situations. The fast fading of the wideband received power in a given environment is reduced with increasing system bandwidth because multipath gain can be exploited by wideband systems. However, the problem of intersymbol interference is increasing with bandwidth. In Fig. 2.6 the cumulative distributions and the standard deviations of the received power levels are shown for three different bandwidths. These curves were evaluated from micro cellular NLOS measurements.

2.3.8 Results for frequency selectivity in different environments

The frequency selectivity of the channel was evaluated from wideband measurements. It was characterised by different parameters, e.g., delay spread, delay window (see Section 2.1.5), interference ratio, notch depth. The largest frequency selectivity have been observed in Alpine regions [99, 100] and mountainous coastal districts, especially in Norwegian and Faroese fjords [97, 98, 60].

The statistical distribution of the delay spreads results in 9th decile values as high as about 10 µs. The delay windows containing 90% of the total signal energy of the impulse responses reach 9th-decentile values of up to 35 µs. Careful selection of base station sites, antenna heights and antenna radiation patterns, e.g., directional antennas or down-tilt patterns are means to reduce the frequency selectivity in this specific environment. The frequency selectivity of the mobile radio channel is significantly lower for rural areas in flat terrain and areas characterised by rolling hills. The 9th deciles of the delay spread distributions are much smaller than 5 µs and the delay windows do not exceed a length of about 12 µs in 90% of the locations.

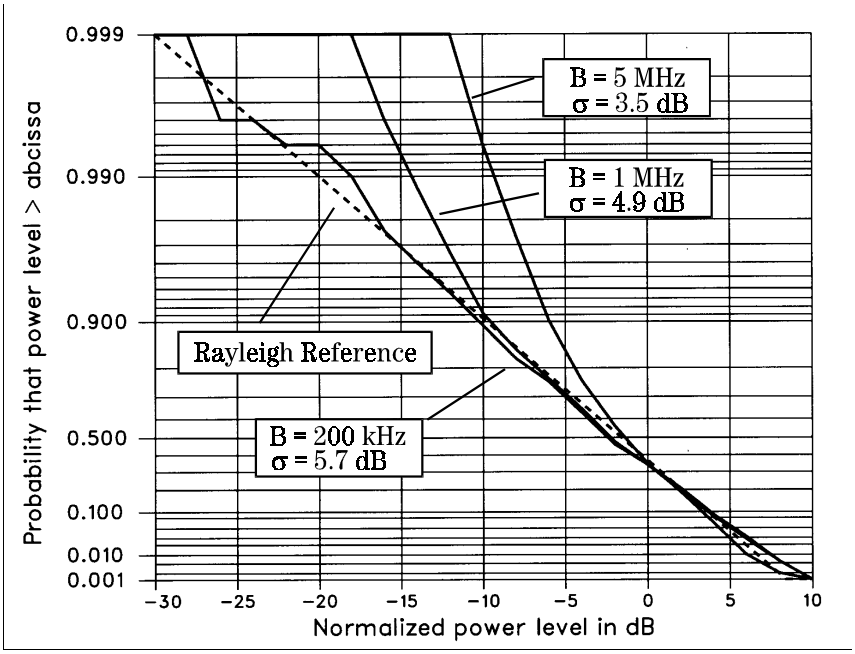

Fig. 2.6 Cumulative distributions of received power levels for 5 MHz, 1 MHz and 200 kHz bandwidth, evaluated from a micro cellular NLOS measurement.

A large variation of the duration of impulse responses was also observed in urban areas characterised by dense, inhomogeneous building structures. Very short as well as rather long excess delays occur. Delay windows larger than 20 µs have been measured where the direct path is heavily obstructed and a good view towards prominent reflectors exists from the base station as well as from the mobile station.

The frequency selectivity as function of the cell size and base station antenna height was investigated. A reduction of the delay spreads from 5 µs to 1.7 µs was noticed when the cell radius was reduced from 3 km to 600 m. If base-station antenna heights are reduced from above to below roof-top levels, an increase of the path loss was obtained, while the delay spread did not change significantly. The analysis of the shape of the power delay profiles resulted in increased attenuation of the direct path with decreasing antenna height while the delayed portions of the impulse responses scattered by prominent reflectors remain approximately unchanged. This phenomenon explains also the drawbacks of path-loss models which take into account only the direct path especially if they are applied to antenna heights below roof-top levels.

In micro cells the delay spread for LOS situations is in the range between 20 ns for small street canyons and 200 ns for large squares. For micro cellular NLOS conditions the delay spread is significantly larger. It may exceed values of 1 µs. The

comparison of the measurements gained in the 900-MHz and the 1800-MHz bands showed that in general no difference between frequency selectivity in the two frequency ranges has to be expected.

2.3.9 Determination of directions-of-arrival (DOA)

In order to obtain a better understanding of the propagation mechanism and to test advanced propagation models, e.g., ray tracing techniques, evaluations of the DOAs of the received signals at different delays were performed. DOAs were determined on the basis of measurements realising a synthetic antenna array (linear, circular, matrix, etc.) [93]. From wideband measurements, the DOA analysis in connection with the excess delay information and in connection with digital terrain information was used to identify scatterer locations. If only power delay profiles are available, scatterer locations can also be estimated from the evolution of the excess delays versus a certain run length. A synthetic aperture antenna, realised by two-dimensional mechanical motion of a scanning antenna mounted on the roof of a van, was used for the determination of the angle-of-arrival distribution at the mobile. Alternatively, the DOAs have been estimated from the evaluation of delay-Doppler scattering function (Eq. (2.20)), processed from impulse responses measured at a spatial separation less than half of a wavelength.

In Fig. 2.7 the delay-Doppler scattering function evaluated from a wideband micro cellular propagation measurement in a NLOS situation is plotted [96]. It can be recognised that the DOAs are widely spread for the different excess delays.

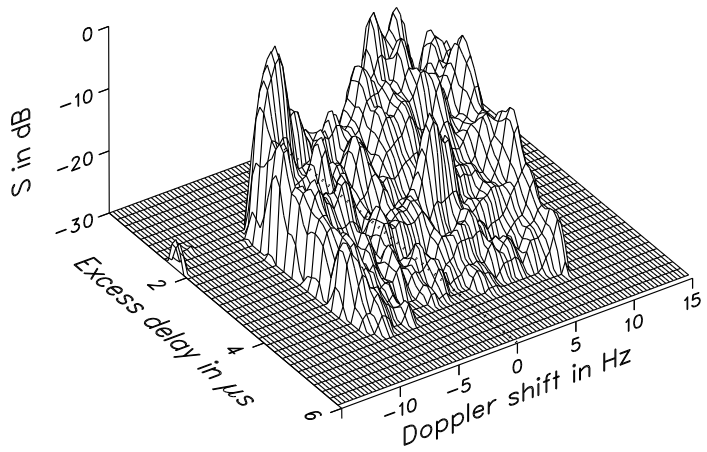

Fig. 2.7 Delay-Doppler scattering function for a micro cellular NLOS situation.

The evaluation of DOAs from delay-Doppler scattering functions needs no extra measurement facilities, but it is restricted by a left-right ambiguity of the DOAs, because it is based only on a one-dimensional scanning of the received radio waves. DOAs of the direct path are often widespread due to scattering in the vicinity of the mobile whereas distant echoes arrive within a smaller angular distribution, e.g., as result of waves guided within a street canyon. The locations and reflection coefficients of scatterers in the terrain can be estimated from the DOAs and excess delays in case of reasonable free line-of-sight to the scatterers. This is a useful method to improve prediction methods which use terrain data bases.

A large DOA measurement campaign using mechanically rotated antenna has been used by [118]; for further details see section 3.2.

2.4 Propagation Modelling for the Simulation of the Radio Channel

Jose Jimenez and Victor Perez, Telefonica I+D, Spain

2.4.1 Radio Channel Simulation

Radio channel characterisation is an essential element in the design and testing of any communication system. Since computer simulation techniques are the most common way of checking performance, it is not surprising that channel characterisation plays a central role in COST 231 activities. A large number of contributions include a section on the channel model used for simulation. In a second phase, adjustment and testing play also an essential role. The design and implementation of a circuit element which mimics channel behaviour (channel emulator) is also a basic step in the design and optimisation process.

The radio propagation channel can be envisaged as an element transforming input signals into output signals. It can be considered as a filter but with time varying characteristics. Mathematically, the response *y(t)* of this element to an input signal *x(t)* can be described as the convolution integral

$$y(t) = \int_{-\infty}^{\infty} x(t-\tau) \cdot h(t,\tau) \cdot d\tau \qquad (2.36)$$

being $h(t,\tau)$ the channel impulse response, where t is the conventional time dimension which gives the variability of the impulse responses, and τ the time delay which characterises the dispersion of the environment. Different approaches are possible to find such an element. The more direct is to provide a collection of "Stored Channels" based on actually measured impulse response characteristics representing the situation

on a specific environment. The second, is to use a Synthetic Channel Model based on the behaviour of the propagation process. The first, which has the advantage of the evident relation to reality, can be inadequate due to the complexity and also to the distortion introduced in the measuring and storing process. The second will only be as good as the theory behind it.

In any case, the simulation of the radio channel has to be considered from a system point of view. A narrowband system requires a different simulation method than a wideband one. Furthermore, the simulation of some system aspects leads to employ

different radio channel approaches, for example, a diversity performance analysis, uses a different model than that employed for the optimum evaluation of the parameters for a modulation scheme. Taking this fact into account, in general terms, simulations within COST 231 have aimed at the following objectives:

- *Long term area simulations*. This has been the case of studies to evaluate signalling performances, coverage studies, cellular efficiency, etc. This type of simulation usually employs simple channels with attenuators. They are modelled by means of a simple dependence with the transceiver position.
- *Narrowband system simulations*. Those studies consider transceiver performance rather than overall system performance, and have been very frequent in the COST 231, for example for the evaluation of new modulation techniques, optimised transceiver architectures, and of singular importance, some simple studies of DECT performance, use of diversity, etc. In those cases, relatively simple AWGN, Rayleigh or Ricean channels are commonly employed
- *Wideband system simulations*. This is the most interesting case, and frequently, the tapped delay channel has been employed. There is a large variety in complexity depending on the use: from the simpler two path Rayleigh channel to the very elaborate models proposed for UMTS simulations.

This section is mainly focused in simulation for the third case. The analysis is concentrated in systems operating in the 900 MHz and 1800 MHz band, leaving for a different chapter the consideration of Broadband systems, including wideband LAN.

2.4.2 Long term area simulations

In order to test general system features, such as system capacity, or the performance and consistency of signalling or power control schemes, it is frequent to employ a conceptually simple deployment scheme. The propagation channel is modelled as an attenuator which depends, among other parameters, on the distance TX-RX, and that intends to predict the average field. A log-normal random variability is usually added

to emulate the effects of shadowing. This very simple scheme is complicated, in more elaborate programming, by consideration of the environment layout, particularly when calculating the capacity and performance results over indoors or microcell environments. This has been the case for the comparison of the ATDMA and CODIT projects performed in SIG5 "Special Interest Group 5 Common Testing Requirements" [103].

There is a relative large number of researchers using tools of this type, most of them working over regular and indefinite planes, as for example the simulation package Cellsim, which follows essentially the structure described above. It has been employed for DECT evaluation studies in indoor scenarios, GSM cellular capacity evaluation, and CDMA. Recent adaptations of the tool have been utilised for UMTS. There are also some commercial packages (Opnet, Bones) which could be adapted for that type of simulation.

2.4.3 Narrowband system simulations

For initial testing of modulation schemes or new access techniques, two basic approaches have been taken: 1) Use of the AWGN model, and 2) Use of a Rayleigh or Ricean Channel (with only 1 tap). Those channel models are very simple but effective for initial analysis and they have been frequently used in academic research inside COST 231. However, though in mobile environments the second one responds more adequately to reality than the first one, they are appropriate only for narrowband systems, hence for most of the systems that have been studied during the COST 231 action, they are incomplete and require to introduce time delay dispersion (wideband) effects.

2.4.4 Wideband system simulations

Simple wideband simulation - 2 path Rayleigh model. A more elaborate model than the narrowband approach uses a two (rarely three) path simulation (equation 2.37), usually each path having Rayleigh (or Rice) statistics. This model is usually sufficient for many cases and has been extensively employed through COST 231, specially for optimisation and evaluation of MSK and GMSK modulation schemes, but also for OFDM, M-PSK, M-QAM, CPM and TCM. It has also been used for the analysis of CDMA access techniques, (use of Joint Detection, Interference Cancellation, etc.). The number of COST 231 references would be very extensive.

$$h(t,\tau) = a_0(t)\cdot\delta(\tau) + a_1(t)\cdot\delta(\tau-\tau_1) \qquad (2.37)$$

This model is also the favourite for the DECT system evaluation, which has been object of extensive studies in COST 231. The use of a 6 taps delay line channel emulator has also been normal during the COST 231 research activities.

WSSUS models. When a detailed investigation of a communication system is required, the channel is simulated by means of a time varying filter, in fact, a generalisation of the two (to six) path models mentioned above. The theory of time

varying filters has been developed originally by Zadeh, but it is in a paper by Bello [8], where the Wide Sense Stationary Uncorrelated Scattering model (WSSUS) is introduced and analysed. This model is fully determined by a two dimensional scattering function in terms of the echo delay τ due to multipath and the Doppler frequency f_d due to the mobile movement.

Software simulation. Implementation aspects. The search for an effective simulation approach is summarised in [104]. In that work, instead of the conventional formula,

$$h(t,\tau)=\sum_{n=1}^{N}\beta_n(t)\cdot e^{j\phi_n(t)}\cdot\delta\left(\tau-\tau_n(t)\right) \tag{2.38}$$

which is directly translated into a filter, and where the measured impulse response functions allow directly to define the random variables β_n, ϕ_n and τ_n, an alternative formulation is obtained, where the scattering function can be used by considering the marginal pdf's of the delay τ, and Doppler f_d functions, obtained from the measured characteristics:

$$h(t,\tau)=\lim_{N\to\infty}\frac{1}{\sqrt{N}}\sum_{n=1}^{N}e^{j\left(\phi_n+2\pi f_{Dn}t\right)}\cdot\delta\left(\tau-\tau_n\right) \tag{2.39}$$

This approach seems to be simpler and more economic in computational terms, though it is not so easily connected to the more intuitive "filter like" realisation. Most of the practical models make use, however, of the equation 2.38, which allows to implement the convolution of the signal with the impulse response functions by means of a FIR filter. There exist different alternatives to get the coefficients (delays and complex amplitudes) of the filter, and have been commented in the introduction. When an extensive provision of measurements is available, the functions may be processed and converted in "Stored Channels" to be used by the FIR. The advantage is clear: the fidelity to a real situation. However, the drawback is that the simulations are limited in the length (as the measurement is), the behaviour is not easy to control, and the dependence with measurements may become onerous.

More frequent is the usage of "Synthetic Models", where the measurements are utilised to get typical parameters for the simulations. With this technique, some fidelity in the emulation of the real channels may be lost, but on the contrary, the main drawbacks of the usage of "Stored Channels" is overcome. The main objective of a synthetic model is usually to get the complex coefficients of the FIR filter in real time, i.e. following a given Doppler spectrum pattern. For this purpose, different alternatives can be envisaged: the first is the classical and widely used method of low-pass filtering two in-quadrature AWGN sequences, in order to get a Rayleigh process with the expected Doppler variation (Classical, Gaussian), like in the COST 207 approach. Another method is based on the interference of phasors obtained randomly from given distributions based on the physical phenomenon, like in the RACE CODIT project [105] (see equation 2.40). Finally, the literature offers other methods

like the one proposed in [106] , aimed at a more accurate description of the Doppler spectrum by using fast Fourier algorithms. Regardless of the method used, there are other aspects to take into account in the implementation of a simulator (HW or SW). The time variant complex impulse response functions defined in equation 2.36 cannot be used directly due to the discrete nature of a digital filtering process. This fact is important for designing simulators with tapped delay lines (FIR filters). Generally speaking, some aspects must be taken into account when treating with these functions, and are originated by the limited number of taps, the bandwidth of the signal, the normalisation of the filter coefficients and the interpolation technique of these coefficients.

For some applications, the channel has to be power normalised in order to keep the signal mean power after a convolution process. This is necessary, for example in AWGN simulations, where the noise power is calculated as a fraction of the signal. The normalisation is achieved in a "natural" way if the scatterers that contribute to the impulse responses are uncorrelated and the sum of their powers equals 1 [105]. However, when a tapped delay line like the one shown in the figure 2.8 is used, it is also required that the coefficients $g_n(t)$ are obtained adequately.

This scheme introduces delays at a rate 1/T equal to the signal sampling rate, therefore it requires a bandlimited filter with a bandwidth greater than or equal to the one of the signal. The coefficients must be obtained from formulas like 2.38, 2.39 or 2.41, which are actually non bandlimited, by a low-pass filtering and sampling.

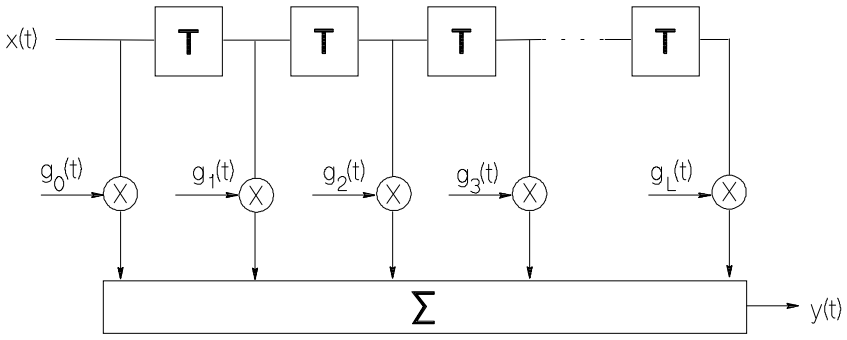

Figure 2.8 FIR filter implementation of a channel simulator

Ideal low-pass filtering, i.e. the use of a sync function yields an infinite number of coefficients, which is not feasible. In practice, for most of the power delay profiles the energy is concentrated in a few number of taps, therefore, if an adequate truncation of the coefficients is performed, the channel function will behave as expected and the power normalisation will be achieved. However, it has to be kept in mind that the truncation depends on the autocorrelation characteristics of the input signal and the

number of side lobes considered, and can affect seriously to the accuracy of the results [105].

There exists a different and easy approach for obtaining a correct normalisation of the output signal, which consists on performing a previous measurement of the mean power by running the simulation with much lower sampling rates for the overall simulation length.

Other aspect that may influence in the final results, is related to the kind of interpolation used to update the coefficients of the filter. As the maximum Doppler deviation is usually much smaller than the sampling rate of the system 1/T, the coefficients are calculated only every KT seconds, i.e. the values at the system sampling rate are interpolated. It has been proved that for practical situations, a linear interpolation allows to get a good accuracy [105].

Other approaches. Other approaches consist in building a Time Frequency Linear Filter. The process uses frequency responses measurements instead of impulse responses. More recently a procedure to rationalise the otherwise somewhat heuristic process for the generation of the WSSUS model based on measurement has been proposed in [107,108] and its findings reported and discussed within COST. The procedure uses the collected measurements and follows a well defined algorithm to determine both the number and characteristics of the taps used in the equivalent transversal filter. In some cases, most usually when high frequencies are involved but also for DECT analysis, a ray tracing model is used. This type of model is very frequent for coverage prediction but has also been used for simulation and performance evaluation for wideband systems in some cases. Generally a very simple (square room) structure is proposed. The received signal is composed of the -several - rays starting at the emitter and ending at the receiver. This procedure also allows for the inclusion of the rays delays. Furthermore, there is considerable work in some issues, varying from the definition of better simulation approaches, to the analysis of the applicability of WSSUS assumptions in some environments. In this area, there has been some interest to overcome some of the theoretical limitations of the WSSUS model, particularly as connected to indoor environments, where the validity may be discussed due to the near-field effects of the antennas, the small dimensions of most of the objects, the intrinsic deterministic characteristics of the man-made structures, etc.[109]. Directly applicable are the investigations on the suitability of the WSSUS model when the mobile has not a constant velocity. Several movement patterns are proposed and analysed in [110]. The conclusions suggest that the use of the WSSUS model in -particularly- indoor environments, may be quite risky. This aspect has also been considered in the CODIT project, where a collection of modulation formulas are suggested to simulate varying environments, particularly for corner crossings.

2.4.5 UMTS simulators

The development of UMTS (RACE II projects) required a more detailed description of the wideband channel, than the one suggested by COST 207 Action for the GSM

system. Two projects, ATDMA and CODIT, devoted some efforts to the definition of new propagation models. Since close contact between those projects and COST 231 Action has been established, a summary of the simulation models is given in this subsection.

COST 207 approach. As indicated, WSSUS models are the most frequently employed in COST 231. The models actually employed depended mostly on the relative bandwidth of the system as compared to the delay spread. The starting point for COST 231 has been the wideband models proposed by COST 207 for the GSM system [13]. That model has proved to be very powerful and, at the same time very simple to use, because it consists of a few figures which are easily provided for simulation. COST 207 provided a collection of suggested channels for testing rural and urban (hilly and non hilly) environments, with implementations of 6 or 12 taps. The basic elements (settings) for the channel simulation are:

- Tap delay values following different profiles.
- Tap mean power and Rayleigh distribution (eventually, for the first ray, a Rice distribution is used).
- Doppler Spectrum types (4): Classical [16], Gaussian (two different types) and Rice (Classical + Direct ray).

GSM COST 207 models have been used as a reference for many measurements and utilised to perform a large amount of theoretical and performance studies. Their applicability is not restricted to GSM but they also have been used for analysing different modulation techniques, access schemes and for the study of diversity. There has been some work presented in the Action on the original GSM channels - to correct mistakes and to clarify some points -, and during the time span of COST 231, new sets of parameters based on measurements have been produced. For example, a very comprehensive measurement campaign, performed by the Norwegian Administration has produced new parameters, following the rules of COST 207, for smoothly rolling farmland, rolling farmland and forest, valleys, mountainous areas and fjords, coastal terrain, suburban and urban terrain. COST 207 models have also been introduced into a number of commercially available simulation tools (COSSAP, SPW).

There has also been some research on the applicability of COST 207 models to the investigation of SFH gain in ATDMA environments. Those studies show a number of difficulties when a six tap model is used for the evaluation of large band effects, such as frequency hopping. The problem is the frequency correlation of the channel which is distinctly different in the model and in measurements. This opens a new research area not covered for the moment.

ATDMA simulator. ATDMA [111] followed two complementary approaches, mentioned above: Stored Measured Channels and Synthetic Channels. For every scenario (indoors, micro and macro cell) a large number of measurements were driven (more than 500 files in some cases) leading to the definition of a *typical channel* and a

collection of (two or three) *atypical channels***.** Those recorded responses can be used either directly -stored channels- or by means of synthetic channels.

The synthetic channels are defined in similar terms of those of COST 207 but, instead of using a standard filter (Class) for the description of the Doppler spectrum, a stored function -based on actual measurements- is produced.

CODIT simulator. CODIT [105, 112] has based its initial work on some theoretical studies and measurements reported in [113,114]. CODIT activities were mostly aimed at the development of a synthetic model for WSSUS. The model was then extended to non-WSSUS scenarios, by means of some modulating functions in the filter coefficients. For the WSSUS, the *scattering function* modelling was utilised as starting point. A large number of scattering functions were analysed and a comprehensive environment classification produced. Even though CODIT uses the conventional FIR approach, both the statistics of the amplitude and Doppler Spectrum of the coefficients are different from those used in COST 207. The simulation of those parameters also differs since they are not based on a filtering process but on a Montecarlo simulation. Every scatterer laid in a given environment will contribute to the total field perceived at a given spatial location in a given time with a number N_{waves} of scattered waves, each of which is characterised by its amplitude a_{il}, its phase deviation φ_{il}, and the angle of incidence of the wave relative to the velocity vector of the mobile, α_{il}. Some other parameters are involved such as the wavelength of transmission, the time *t*, and the vehicle speed *v*. The total contribution due to the i-th scatterer looks like

$$E_{si}(t) = a_{io} \cdot e^{j\left(\varphi_{io}+\frac{2\pi}{\lambda}vt\cdot\cos(\alpha_{io})\right)} + \sum_{l=1}^{N} a_{il} \cdot e^{j\left(\varphi_{il}+\frac{2\pi}{\lambda}vt\cdot\cos(\alpha_{il})\right)} \quad (2.40)$$

The total field perceived at a given spatial location in a given time can be obtained as the addition of the contributions due to every scatterer. The contributions of *M* scatterers travelling through radioelectrical paths of different lengths will not arrive aligned in time, but exhibiting a certain delay (time dispersion) with respect to the line-of-sight ray:

$$h(t,\tau) = \sum_{i=1}^{M} E_{si}(t) \cdot \delta(\tau - \tau_i) \quad (2.41)$$

2.4.6 Hardware Channel simulators

There has been relatively less activity in the hardware simulation front. Most contributions in this area have been based on acceptance test reports. As an example,

several channel emulators designed to emulate dual GSM channels as defined in GSM 05.05 [115], were reported inside the Action. Those acceptance tests have been useful not only for the manufacturing company, but also for other groups working in COST 231. The study of the DECT system was sometimes performed by means of channel emulators, complemented by actual measurements with a laboratory equipment that could generate time dispersed signals. The essential idea was to utilise tap delay lines with transmitting antennas. Other researchers employed controlled propagation areas where reflectors were carefully located. This kind of work can be better dealt under system evaluation or in -controlled- field test. A digital hardware quadrature baseband sounder based on fast FIR-processors has been developed by Aalborg University [119], with a throughput bandwidth of 1.2 MHz. The different Doppler spectra associated with each FIR tab are down-loadable from a PC. Due to this flexible approach, both simulated and measured (stored channel) Doppler spectra can be used.

ATDMA and CODIT have developed hardware channel simulators for use in their real time testbeds. They have been designed using a time variant transversal filter. The filter coefficients, in the CODIT case, are simulated with the process described above instead of using the conventional Rayleigh filtering technique. ATDMA relies on the use of stored channels, besides to the capability of generating synthetic responses.

CODIT channel emulator. This channel emulator has been designed for coping with most of the UMTS environments, thus it is able to work in different propagation conditions - different power delay profiles - with high bit rates.

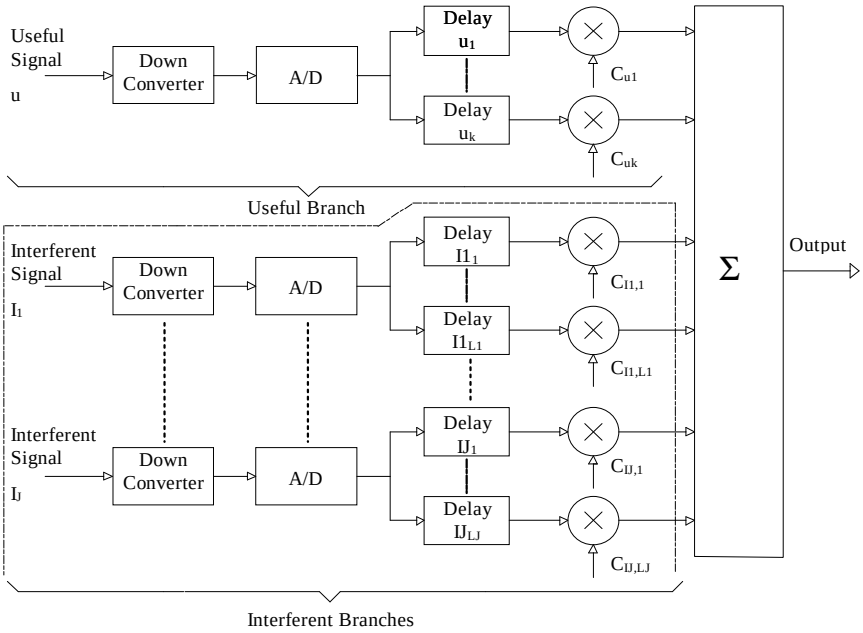

Figure 2.9 General structure of the CODIT Channel Emulator

The main characteristic is the flexibility, which provides the capability to emulate both outdoor and indoor environments and co-channel interfering signals (this is compulsory in a CDMA system) affected by different or equal channel models. A schematic diagram of the FIR filter is shown in Fig. 2.9.

A FIFO memory is introduced in every tap branch simulating a programmable tap delay line, in order to keep the ability to emulate very different channel behaviours with a limited number of different tap branches. Two circuits (besides the RF stages) are identified:

- *Control circuit.* By means of multiplexer circuits, the signals are selectively introduced in one of the J+1 available branches (different filters), each one comprising L_i taps. This allows to set the filter structure as function of the inputs used: if there are J interfering signals, and the total number of available taps is N, the useful signal will have ($N-L_1-L_2-...L_J$) assigned taps. The CODIT channel emulator has 20 taps, 3 inputs and 2 outputs (to provide up and down link simultaneously), thus up to 2 interfering signals can be used with 6 possible branches.
- *Basic tap circuit.* To guarantee that all the filter coefficients which are computed in a sequential way in the DSP processor change simultaneously, a latch circuit has been introduced in every tap. These coefficients are fed to a FIFO memory from a file generated by adequate software tools, and then are real time interpolated by the DSP processor. A complex multiplier completes the tap circuit.

2.5 References

[1] T. Bull, M. Barrett, R. Arnott, "Technology in smart antennas for universal advanced mobile infrastructure (TSUNAMI) - an overview", in *Proc. of the RACE Mobile Communications Summit*, (Cascais, Portugal), (Nov. 22-24), pp. 88-97, 1995.

[2] D. J. Cichon, "Ray optical modelling of wave-propagatiojn in urban micor and pico cells" (in German : "Strahlenoptische Modellierung der Wellenausbreitung in urbanen Mikro- und Pikofunkzellen"), in *Forschungsberichte aus dem Institut fuer Hoechstfrequenztechnik und Elektronik der Universitaet Karlsruhe*, vol. 8, ISSN 0942-2935, Ph.D. Thesis, University of Karlsruhe, Faculty of Electrical Engineering, 1994.

[3] B. Fleury, D. Dahlhaus, "Investigations on the time variations of the wide-band radio channel for random receiver movements", in *Proc. of the IEEE Third Int. Symp. on Spread Spectrum Techniques and Applications (ISSSTA '94)*, (Oulu, Finland), pp. 631-636, July 1994.

[4] T. Huschka, "Correlations of time-variant impulse responses in an indoor environment", in *Proc. IEEE Vehicular Techn. Conf. VTC' 95*, (Chicago), 1995.

[5] *COST 231 TD(89) 030* L. Olsson, "On the fading of radiowaves above 0.5 GHz indoor"

[6] D. C. Cox, "Antenna diversity performance in mitigating the effects of portable radio telephone orientation and multipath propagation", *IEEE Trans. Commun.*, vol. COM-31, pp. 620-628, May 1983.

[7] P. Melancon and J. Lebel, "Effects of fluorescent lights on signal fading characteristics for indoor radio channels", *Electronics Letters*, vol. 28, pp. 1740-1741, Aug. 1992.

[8] P.A. Bello, "Characterization of randomly time-variant linear channels", *IEEE Trans. Commun. Syst.*, vol. CS-11, pp. 360-393, Dec. 1963.

[9] I. I. Gihman and A. V. Skorohod, *The Theory of Stochastic Processes*. Springer, 1974.

[10] S. L. Lauritzen, C. Thommesen, and J. Bach Andersen, "A stochastic model in mobile communications", *Stochastic Processes and their Applications*, vol. 36, pp. 165-172, 1990.

[11] R. Collin, F. Zucker, *Antenna Theory*, vol. 1, McGraw Hill, 1969.

[12] J. Bach Andersen, P. Eggers, "A heuristic model of power delay profiles in landmobile communications", in *Proc. URSI Symposium on Electromagnetic Theory*, (Sydney, Australia), pp. 55-57, Aug. 1992.

[13] J.-P. de Weck, J. Ruprecht, B. Nemsic, H. Bühler, "Sounding radio channels for 1.8 GHz personal communications systems", in *Proc. VTC '92*, Denver Col., USA, May 10-12, 1992, pp. 490-493.

[14] A. F. Molisch, "Statistical properties of the RMS delay spread of mobile radio channels with independent Rayleigh-fading paths", *IEEE Trans. Veh. Technol.*, Feb. 1996.

[15] B. Fleury, “An uncertainty relation for WSS processes with an application to WSSUS systems”, *IEEE Tran. Commun*., (Accepted for publication).

[16] W. C. Jakes, ed., *Microwave Mobile Communications*. New York: John Wiley & Sons, 1974.

[17] Matthews P.A., Mohebbi B. : "Direction of Arrival and Building Scatter at UHF", Proc. ICAP 91, Part 1, pp. 147 - 150, 1991

[18] *COST 231 TD(91)035* Antti Koivumaki “Direction Diversity Measurements at 900 MHz”

[19] *COST 231 TD (92)0 24* A. Lévy "Time Structures of the Urban Mobile Channel"

[20] *COST 231 TD(92)061* Jaakko Lähteenmäki “High-resolution Direction-of-arrival measurements”

[21] *COST 231 TD(92)065* P.A. Matthews and A. Hairi Abu Bakar “Direction of arrival of radio signals within buildings”

[22] *COST 231 TD(90)028* Jenss Jakobsen “Radio Propagation Measurements in two Office Buildings”

[23] *COST 231 TD(90)039* Jaakko Lähteenmäki “Measurements and Modelling for Indoor Power Delay Profile”

[24] *COST 231 TD(91)034* Jaakko Lähteenmäki “More Wide-Band Measurements at 1.7 GHz”

[25] *COST 231 TD(91)0 29* P.C. Andersen et al. “Delay Spread Measurements at 2 GHz”

[26] *COST 231 TD(93)097* U. Kauschke " Wideband Path Loss and Delay Spread Measurements in a NLOS situation"

[27] Kauschke U. : "Wideband Indoor Channel Measurements for DECT Transmitter Positioned Inside and Outside Office Buildinds", Proc. PIMRC'94 and WIN, The Hague Sept. 1994, Vol. IV pp 1070 - 1074

[28] *COST 231 TD(94)013* F. Jimenez, J.M. Hernando, R. Herradon "Wideband and Narrowband characterization in microcellular and picocellular environments"

[29] *COST 231 TD(89)0 41* “ Real-Time Channel Sounder (RCSS 900)”

[30] de Weck J.P., Ruprecht J. "Real-time ML estimation of very frequency-selective multipath channels", Proceedings GLOBECOM'90, vol. 3, pp 2045-2050, 1990

[31] Berg J.E., Mattson A., Ruprecht J. and de Weck J.P., "Specular reflections from high-rise buildings in 900 MHz cellular systems, "Proceedings of the 41st IEEE Veh. Technology, 1991

[32] *COST 231 TD(95)030* J. Ruprecht, H. Bühler, T. Klemenschits " Universal Channel Analyser: a Hardware/software Concept to measure and Analyse Mobile radio Channels"

[33] *COST 231 TD(90)014* M. J. Devasirvatham “Multi-Frequency Radiowave Propagation Measurements in the Portable Radio Environment”

[34] *COST 231 TD(92)122* P.E. Mogensen “Wideband Polarization Diversity Measurements for Wireless Personal Radio communications”

[35] *COST 231 TD(93)008* P. Eggers, J. Toftgard “Initial results on wideband base-station antenna diversity for in-and outdoor pico-cell environments”

[36] Gürdenli E., Huisch P.W. : "Propagation measurements and modelling for digital cellular radio systems", British Telecom Technical Journal, vol. 8, N° 1, pp. 44-56, Jan.

[37] *COST 231 TD(94)080* P. Karlsson, L. Olsson "Time Dispersion Measurement System for Radio Propagation at 1800 MHz and Results from Typical Indoor Measurements"

[38] *COST 231 TD(90)009* “ Real-Time ML-Estimation of very Frequency-Selective Multipath Channels”

[39] *COST 231 TD(94)019* J. Jimenez "Propagation activities and simulation models in CODIT (RACE 2020) project"

[40] *COST 231 TD(94)068* M. Grigat "Wideband measurement techniques and data evaluation"

[41] Barbot J.P., Bic J.C., Gollreiter R., Grigat M., Kadel G., Lévy A.J., Lorenz R.W., Mohr W.,Strasser G. : Channel Characterization for Advanced TDMA Mobile Access", Proc. Race Mobile Telecommunications Workshop, Metz 1993, pp. 378 -384

[42] Kadel G., Lorenz R.W. : "Wideband propagation measurements of the mobile radio channel", Proc. ISAP' 92 Sapporo 1992, pp. 81-84

[43] *COST 231 TD(90)041* R.W. Lorenz “First results of measurements using a digital channel sounder with a bandwidth matched to the GSM system”

[44] *COST 231TD(90)075* R.W Lorenz, G. Kadel " Evaluation of propagation measurements using RUSK 400, a digital- sounder matched to the GSM bandwidth"

[45] Martin U., Reng R., Schüssler H.W. and Schwarz K., : "Determination of wideband impulse responses", Proc. URSI International Symposium on Signals Systems and Electronics 1989, pp. 393-396

[46] Hermann H., Martin U., Reng R., Schüssler H.W. and Schwarz K., : "High resolution channel measurement for mobile radio", Proc. EUSIPCO-90 Conference, Barcelona Sept.1990, pp. 1903-1906

[47] Kauschke U. : "Propagation Measurements with RUSK SX and Simulations for a typical DECT Scenario in Urban Streets", Proc. 2nd Joint COST 227/231 Workshop on Mobile and Personal Com. Florence, April 1995, pp. 255-266

[48] *COST 231 TD(95)021* J. Wiart, P. Pajusco, A. Lévy, J.C. Bic "Analysis of Microcellulars Wideband Measurements in Paris"

[49] Levy A.J., Rossi J.P., Barbot J.P. and J. Martin, “An improved channel sounding technique applied to wideband mobile 900 MHz propagation measurments”, Proc. of the 40th IEEE Vehicular Technology Conference, Orlando 1990

[50] E. Zollinger, "Measured inhouse radio wave propagation characteristics for wideband communication systems", 8 th European Conference on Electrotechnics, EUROCON'88, pp 314-317, June 13-17, 1988; Stockholm, Sweden

[51] A. Radovic, E. Zollinger, "Measured time-variant characteristics of radio channels in the indoor environment, "Mobile Radio Conference 1991, MRC'91, pp 267-274, November 13-15, 1991, Nice, France.

[52] E. Zollinger, "Verfahren zur Bestimmung der komplexen Enveloppe von Eingangszeitdispersionsfunktionen linearer, zeitvarianter Zweitore" *(Method for the determination of the complex envelope of the impulse response of linear, time-variant two-port networks)*, Patentanmeldung, Amtl. Aktenzeichen : 3431/91-1, November 22, 1991, ASCOM Tech AG, Bern.

[53] E. Zollinger, "Indoor wave propagation and analysis techniques", Workshop WMFG on "Field Theoretical Problems for Wireless Technology", 1995 IEEE MTT-S International Symposium, May 15, 1995, Orlando, FL, USA.

[54] P. de Weeck, P. Merki, R. Klingler, A. Radovic, E. Zollinger and U. Dersch (Editor J.F. Wagen), "Wideband mobile radio channel measurement and modelling", International Commsphere'91 Symposium, pp. 8.1.1-8.1-10, Dec. 15-19, 1991, Herzliya, Israel.

[55] E. Zollinger, “Methods for determining complex envelopes of impulse responses of linear time variant two-ports” (in German : “Verfahren zur Bestimmung der komplexen Enveloppe von Stossantworten linearer, zeitvarianter Zweitore”), Patentschrift A5, CH 682262 A5, August 13, 1993, ASCOM Tech AG, Bern

[56] E. Zollinger, "Methods for measuring mobile radio channels", Tutorial E, 1994 International Zurich Seminar on Digital Communications, March 8-11, 1994, ETH Zurich, Switzerland.

[57] Felhauer T;, Baier P., König W. and Mohr W. : "Optimum Spread Spectrum Signals for Wideband Channel Sounding", Electronics letters, Vol. 29, N° 6, pp. 563-564, March 1993

[58] Felhauer T., Baier P., König W. and Mohr W. : "Optimized Wideband System for Unbiased Mobile Radio Channel Sounding with Periodic Spread Spectrum DSIgnals", IEICE Transactions on Communications, Vol E76-B, N° 8, pp. 1016-1029, August 1993

[59] *COST 231TD (95)128* W. Mohr, B. Steiner, P. Weber "The Siemens Mobile Channel Sounder"

[60] P. Eggers, C. Jensen, A. Oprea, K. Davidsen, M. Danielsen, “Assessment of GSM link quality dependence on radio dispersion in rural environments”, in *Proc. VTC ’92*, Denver Col., USA, May 10-12, 1992, pp. 532-535.

[61] G. Kadel, “Determination of the GSM system performance from wideband propagation measurements”, in *Proc. VTC ’92*, Denver Col., USA, May 10-12, 1992, pp. 540-545.

[62] *COST 231 TD(93)048* Albert Molina, Peter Cullen, Paul Fannin “A Digital Wideband Mobile Radio Channel Sounder”

[63] Molina A., Fannin P; : "Accuracy and Dynamic Range Improvement of Bandpass Impulse Response Measurements with pseudo-random noise", Electronics Letters, Vol. 27, N° 19, Sept. 1991, pp. 1755 - 1756

[64] *COST 231 TD(93)088* R. Gahleitner, Th. Klemenschits, R. Stepanek “First results of a Direct-Conversion channel sounder (DCCS1800) recorded in a road tunnel”

[65] *COST 231 TD(95)005* P. Bartolomé "Wideband Measurements in Outdoor Environments"

[66] *COST 231 TD(90)027* R.H. Rækken “Description of the Norwegian Impulse Response Measurements”

[67] Løvnes G., Paulsen S.E., Rækken R.H. : "Wideband propagation measurements at 900 MHz and 1.7 GHz in macrocells", Proc. ISAP 92, Sapporo, pp. 77-80

[68] Rækken R.H. , Eskedal B.E. : "DECT performance in multipath environments", Proc. Nordic Radio Symposium 1995 (NRS'95), Saltsjobaden, Sweden, April 1995

[69] *COST 231 TD(91)071* S. Ruiz-Boqué et al.“Indoor wideband channel characterization (900 and 1800 MHz) by means of a network analyzer”

[70] *COST 231 TD(930)89* J. Jimenez, M. Pizarroso, V. Perez, U. Dersch "CODIT Measurement Campaign : Wideband Indoor Measurements"

[71] Gollreiter, R. (editor): Channel models Issue 2. RACE ATDMA Document R2084/ESG/CC3/DS/P/029/b1, May 15th, 1994.

[72] P. Bartolomé, "Indoor propagation models validation," *COST 231 Temporary documents*, TD(93)51, Barcelona 1993.

[73] C. Törnevik, J.-E. Berg, F Lotse, "900 MHz propagation measurements and path loss models for different indoor environments," *Proceedings of 43rd IEEE VTC-93,* New Jersey, USA, 1993.

[74] J. Wiart, "Indoor electromagnetic wave propagation measurements and modelling,” *COST 231 Temporary documents*, TD(94)24, Lisbon , January 1994.

[75] P. Karlsson, "Indoor radio propagation for personal communications services," dissertation, University of Lund, 1995

[76] R. Gahleitner, "Radio wave propagation in and into urban buildings," dissertation, Technical University of Vienna, 1994.

[77] S. Ruiz-Boqué, M Ballart, C. Clúa, R Agusti, "Propagation models for indoor mobile communications," *COST 231 Temporary documents,* TD(91)14, Florence 1991.

[78] J. Lähteenmäki, "Radiowave propagation in office buildings and underground halls," *Proc. of European Microwave Conference,* Espoo 1992, pp. 377-382.

[79] P. Karlsson, L. Olsson, "Time dispersion measurement system for radio propagation at 1800 MHz and results from typical indoor environments," Proc. of 44th IEEE Vehicular Technology Conference, 1793-1797, 1994.

[80] U. Dersch, E. Zollinger, “Propagation mechanisms in micro cell and indoor environments,” *Transactions on Vehicular Technology,* Vol. 43, Nov. 1994, No. 4, pp. 1058-1066.

[81] S. Ruiz-Boqé, R. Agusti, J. Peréz, “Indoor wideband channel characterization (900 and 1800 MHz) by means of a network analyzer, *COST 231 Temporary documents*, TD(91)71, Lund 1991.

[82] J. Lähteenmäki, "Determination of dominant signal paths for indoor radio channels at 1,7 GHz," *Proc. of the 4th International Symposium on Personal, Indoor and Mobile Radio Communications*, Yokohama 1993, pp. 392-396.

[83] J. Fuhl, Virtual-Image-Array Single-Snapshot (VIASS) algorithm for direction-of-arrival estimation of coherent signals, COST 231 Temporary Documents, TD(95)23, Bern, January 1995.

[84] A. H. Abubakar and P. A. Matthews, " Direction of arrival of radio signals inside and outside buildings," *Proc. of IEEE 44th Vehicular Technology Conference*, June 8-10, 1994, Stockholm, Sweden, pp. 1754-1756.

[85] U. Dersch, E. Zollinger, "Propagation measurements in micro cell and indoor environments," *The 4th Int. symposium on Personal, Indoor and Mobile Radio Communications (PIMRC'93)*, pp. 191-195, Yokohama, Sept. 8-11, 1993, Japan.

[86] U. Dersch, J. Troger, E. Zollinger, "Multiple reflections of radio waves in a corridor," *IEEE Trans. Antennas and propagation*, vol 42, no. 11, pp. 1571-1574, Nov. 1994.

[87] E. Zollinger, "Indoor wave propagation and analysis techniques," *1995 IEEE MTT-S Int. Symposium, May 15, 1995, Orlando, FL, USA.*

[88] Barbot, J.P., Bic, J.C., Gollreiter, R., Grigat, M., Kadel, G., Levy, A.J., Lorenz, R.W., Mohr, W., Strasser, G.: Channel Characterisation for advanced TDMA Mobile Access. Proceedings of the RACE Mobile Telecommunications Workshop, Metz, 16-18 June 1993, pp. 378-384.

[89] Jakoby, R., Liebenow, U.: Modelling of radiowave propagation in microcells. Proceedings of the 9th International Conference on Antennas and Propagation ICAP'95, Vol. 2, Eindhoven, April 1995, pp. 377-380.

[90] Liebenow, U., Kuhlmann, P.: Theoretical investigations and wideband measurements on wave propagation in hilly terrain. Proceedings of the IEEE Vehicular Technology Conference (VTC), Stockholm 1994, pp. 1803-1806.

[91] Kadel, G. and Lorenz, R.W.: Mobile propagation measurements using a digital channel sounder with a bandwidth matched to the GSM-system. Proceedings of the seventh International Conference on Antennas and Propagation (ICAP 91). IEE Conf. Publ. 333, 1991, pp. 496-499.

[92] Lorenz, R.W. and Kadel, G.: Propagation measurements using a digital channel sounder matched to the GSM-bandwidth. ICC'91, Denver, USA, 1991, pp. 548-552.

[93] Lorenz, R.W. and Kadel, G.: Digital channel sounder for remote sensing of scatterers in mobile radio environment. AGARD Conference Proceedings 502 (1991), pp. 34.1-34.9.

[94] Kadel, G. and Lorenz, R.W.: Wideband propagation measurements of the mobile radio channel. Proceedings of the International Symposium on Antennas and Propagation (ISAP 92). Sapporo 1992, pp. 81-84.

[95] Kadel, G., Lorenz, R.W.: Wideband characterization of the mobile radio channel and its impact on system performance. Abstracts of the XXIVth URSI General Assembly, Kyoto, Japan (1993), p.1.

[96] Kadel, G., Lorenz, R.W.: Impact of the radio channel on the performance of digital mobile communication systems. Proceedings of the Sixth International Symposium on Personal, Indoor and Mobile Communications (PIMRC), Toronto, September 1995, pp. 419-423.

[97] G. Løvnes, S. E. Paulsen and R. H. Rækken: "UHF radio channel characteristics. Part one: Multipath Propagation and Description of the NTR channel sounder", Kjeller, Telenor R&D, 1991, ISBN 82-423-0172-7.

[98] G. Løvnes, S. E. Paulsen and R. H. Rækken: "UHF radio channel characteristics. Part two: Wideband propagation measurements in large cells", Kjeller, Telenor R&D, 1992, ISBN 82-423-0214-6.

[99] Nemsic, B., deWeck, J.-P., Bühler, H., Ergoth, T.: Wideband radio channel characteristics in alpine regions, Electron. Lett. 27 (1991), 717-719.

[100] Nemsic, B., Bühler, H., Bonek, E.: Assessment of wideband radio channels in alpine regions using PICAM, Proc. 41st IEEE Vehicular Techn. Conf., St. Louis, Mai 1991, 491-495.

[101] Bühler, H., Nemsic, B.: PICAM: A PC based cellular network planning software package, Proc. IEEE Mediterr. Electrotechn. Conf. MELECON 91, Ljubljana, Mai 1991, 643-646.

[102] Gahleitner, R., Bonek, E.: 900 and 1800 MHz wave penetration into urban buildings, Proc. XXIVth General Assembly of URSI, Kyoto, Japan, Sept. 1993, 557, paper CBEF-2.

[103] M. Pizarroso, J. Jimenez Ed. “Preliminary Evaluation of ATDMA and CODIT System Concepts”. MPLA/TDE/SIG5/DS/P/001/b1.

[104] P. Hoeher. “A Statistical Discrete Time Model for the WSSUS Multipath Channel”. IEEE Tansactions on VT, vol 41, No. 4, Nov. 1992.

[105] J. Jimenez, V. Pérez, Ed. “Final propagation model” CEC RACE CODIT R2020/TDE/PS/DS/P/040/b1.

[106] P.M. Crespo and J. Jiménez, “Computer Simulation of Radio Channels Using a Harmonic Decomposition Technique”. IEEE Tr. on VT, vol. 44, No. 3, Aug 95.

[107] U. Martin, “Modelling the Mobile Radio Channel by Echo Estimation” Frequenz 48 (1994) 9-10

[108] U Martin, “Echo Estimation - Deriving Simulation Models for the Mobile Radio Channel” Conf. Proc. IEEE VT95 Chicago, July 95.

[109] U. Dersch, “Physical Modelling of Macro, Micro and Inhouse Cell Mobile Radio Channels”, PIMRC Oct. 1992, Boston.

[110] T. Huschka “Correlations of Time Variant Impulse Responses in an Indoor Environment”. Proc. of the 45 IEEE VT Conf, July 1995

[111] R. Gollreiter Ed, “Channel Models. Issue 2”, CEC RACE R2084/ESG/CC3/DS/P/029/b1.

[112] F. Casadevall, A. Gellonch, J. Olmos, G. Femenias. “Channel Emulator for CoDiT project”. RACE Mobile Communications Summit, Cascais, Portugal, Nov. 1995

[113] W.R. Braun, U. Dersch. “A Physical Mobile Radio Channel Model”, IEEE Trans. Veh. Technology. Vol 40, No.2 May. 1991.

[114] U. Dersch and R. Ruegg “Simulation of the time and Frequency Selective Outdoor Mobile Radio Channel”. IEEE Trans. on VT. Vol 42, No. 3, August 1993.

[115] ESTSI prETS 300 577 GSM 05.05, Digital cellular telecommunications system (Phase2); Radio transmission and reception, August 1996, 8th Edition

[116] G. Kadel, “Simulation of the DECT system using wideband channel data measured in two diversity branches”, in *Proc. 2nd Int. Conf. on Univ. Pers. Com*., Ottawa, Canada, Oct. 1993, pp. 546-550

[117] F. Gatti, F. Tallone, “Propagation measurements in wideband mobile channels”, in *Proc. XIII IMEKO World Congress - From Measurement to Innovation*, Turin, Italy, September 1994

[118] P.C.F. Eggers, G.F. Pedersen, K. Olesen, “Multi sensor propagation”, RACE II-TSUNAMI deliverable R2108/AUC/WP3.1/DS/I/046/b1, D.3.1.1., August 1994

[119] S. Pedersen, “Real Time Hardware Radio Channel Simulator”, *in Proc. Nordic Radio Symposium* (NRS’92), Aalborg, Denmark, June 1992, pp. 191-194

[120] P.C.F. Eggers, C. Jensen, A.M. Oprea, “Assessment of GSM-link quality dependence on radio dispersion in rural environments”, in *Proc. Nordic Radio Symposium* (NRS’92), Aalborg, Denmark, June 1992, pp. 19-22

[121] J. Toftgård, P.C.F. Eggers, “Experimental characterization of the polarization state dynamics of personal communication radio channels”, in *Proc. IEEE VTC’93*, Secaucus, NJ, USA, May 1993, pp. 65-69

[122] P.E. Mogensen, P. Eggers, C. Jensen, J. Bach Andersen, “Urban area radio propagation measurements at 955 and 1845 MHz for small and micro cells”, in *Proc. Globecom’91*, Phoenix, AZ, USA, December 1991, pp. 1297-1302